Scientific Voyage
Vol. 1, No. 1,
Page 1-12 (2020)

SCIENTIFIC VOYAGE
ISSN: 2395-5546

ISSN: 2395-5546

Dynamic behavior of PWM Controlled DC drive

Krishnendu Chakrabarty[1] and Urmila Kar[2]

[1] *Electrical Engineering, Government College of Engineering and Ceramic Technology, Kolkata 700 010, West Bengal, India; Email: chakrabarty40@rediffmail.com*

[2] *National Institute of Technical Teachers' Training & Research Kolkata 700106, West Bengal, India*

Abstract: This paper describes bifurcation phenomena of a PWM controlled dc shunt drive. Bifurcation behavior of the system is observed by varying system parameters. The route of transition from periodic behavior to chaos has been investigated and quantified by maximum Lyapunov exponent. The stability of the system is found out using the state transition matrix over one switching cycle (the monodromy matrix) including the state transition matrices during each switching (the saltation matrices). The parameter values at which the nominal period-1 orbit loses stability is determined.

Keywords: Chaos; Bifurcations; DC drive; monodromy matrix; saltation matrix; Lyapunov exponent

1. Introduction

Chaos is an aperiodic long-term behavior of a deterministic system that exhibit sensitive dependence of initial condition. Most of the systems available around us are nonlinear in nature. But much time and energy is spent in understanding a linear system. Moreover, analysis of nonlinear system is also carried out with the help of theory developed for linear systems. This analyses the behavior of a nonlinear system by local linearization. But there are limitations of the analysis of nonlinear system in the light of linear control theory. This approximation fails to reveal actual behavior of the nonlinear system. A fascinating phenomenon of a nonlinear system is the occurrence of chaos. This behavior of a nonlinear system is not due to noise and complexity of the system. It is inherent behavior of a nonlinear system. Chaos theory provides tools to carry out this analysis.

A DC drive is extensively used in the industry. The knowledge of the behavior of the DC drive is of great importance for its proper functioning and design. Since the DC drive is nonlinear in nature, chaos occurs in this system. The occurrence of chaos and routes to chaos has been investigated in the light of chaos theory.

Chau et al. [1] investigated the nonlinear dynamics and chaotic behavior of chopper fed permanent magnet motor drive. Chakrabarty et al. [2-6] reported chaos in dc series drive by numerical simulation. A technique based on Filippov's method of differential inclusion [7] has been employed to analyze the stability of mechanical switching system [8], dc-dc converter [9], full bridge converter fed drive [10] and Photovoltaic system [11].

In this paper, the dynamic behavior of the DC shunt drive has been investigated to find out the dependence of different parameters in the system. Chaotic dynamics of the drive are then discussed. The stability analysis of the period-1 orbit of the drive is performed by the derivation of saltation and monodromy matrices of the system.

2. Mathematical model

The block diagram and equivalent circuit of the DC drive circuit is shown in the Figs. 1and 2 respectively. The output of the speed sensor (W) is compared with the reference speed (W_{ref}) in the comparator A_1. The difference of (W-W_{ref}) is compared with a ramp voltage. The output of the comparator A_2 is used to switch on the switch for the chopper drive. When control voltage exceeds ramp voltage, power switch of the chopper is off and diode is on;

otherwise, the power switch is on and diode is off. The system is linear in nature except the switch. The chaotic behavior of the system is due to switching nonlinearity.

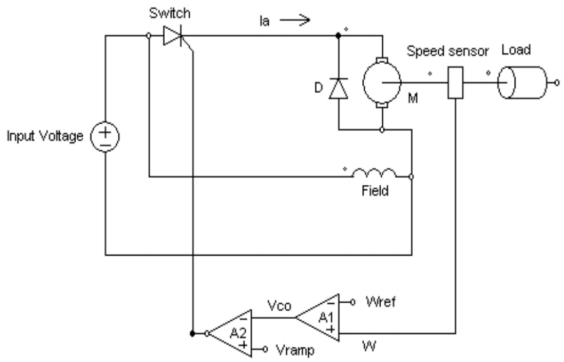

Fig.1: Schematic diagram of DC shunt drive

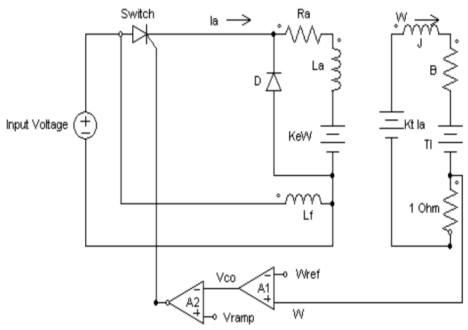

Fig. 2: Equivalent circuit of DC shunt drive

With reference to Fig. 2, i (t) is the armature current, R_a , armature resistance, L_a , armature inductance, V, supply voltage, K_E , back emf constant, K_T , torque constant, B ,viscous damping, J, load inertia and T_l load torque.

The system equations are given by

$$La\frac{di}{dt} = -R_a i - K_E\omega + V$$
$$J\frac{d\omega}{dt} = K_T i - B\omega - T_l \quad (1)$$

Motor speed, ω , is controlled by naturally sampled constant frequency pulse width modulation. The operational amplifier *A1* has gain *G*. The control signal, $V_{co}(t) = G[\omega(t) - \omega_{ref}(t)]$ where, $\omega(t)$ and ω_{ref} are instantaneous motor speed and reference speed respectively, compared with a ramp signal V_{ramp} in the comparator A_2. The ramp is given by $V_{ramp} = V_l + (V_u - V_l)\frac{t}{T}$, where V_u and V_l are upper and lower levels of ramp having period *T*.

The chopper fed shunt motor drive operates in the continuous current mode. The system can be divided into two stages depending on the switching conditions.

The switch will be on when $V_{co}<V_{ramp}$. The corresponding system equations are

$$\frac{d}{dt}\begin{bmatrix} i(t) \\ \omega(t) \end{bmatrix} = \begin{bmatrix} \frac{-Ra}{La} & \frac{-K_E}{La} \\ \frac{K_T}{J} & \frac{-B}{J} \end{bmatrix} \begin{bmatrix} i(t) \\ \omega(t) \end{bmatrix} + \begin{bmatrix} \frac{V}{La} \\ \frac{-T_l}{J} \end{bmatrix} \tag{2}$$

The switch will be off when $V_{co}>V_{ramp}$. The corresponding equations are

$$\frac{d}{dt}\begin{bmatrix} i(t) \\ \omega(t) \end{bmatrix} = \begin{bmatrix} \frac{-Ra}{La} & \frac{-K_E}{La} \\ \frac{K_T}{J} & \frac{-B}{J} \end{bmatrix} \begin{bmatrix} i(t) \\ \omega(t) \end{bmatrix} + \begin{bmatrix} 0 \\ \frac{-T_l}{J} \end{bmatrix} \tag{3}$$

By defining the state vector x(t) and the following matrices A, E_1, E_2, The system can be rewritten as $\dot{x}(t) = Ax(t) + E_K$, where K= 1, 2. K changes the value depending on 'On' or 'Off' condition of the switch. Thus, the closed loop drive system is a second order non-autonomous dynamical system.

3. Bifurcation behavior

In order to study dynamic behavior of the DC drives, parameters of the drive system are as follows: V_l=0, Vu=2.2, T=8ms, G=0.8, Ra=7.8Ω, La=30. mH, B=0.000654,J=0.000971,T_l=0.5 Nm, w_{ref} =100 rad/sec. K_T=0.1324, K_E=0.1356.

The drive has been simulated with SIMULINK of MATLAB as shown in the Fig. 3.

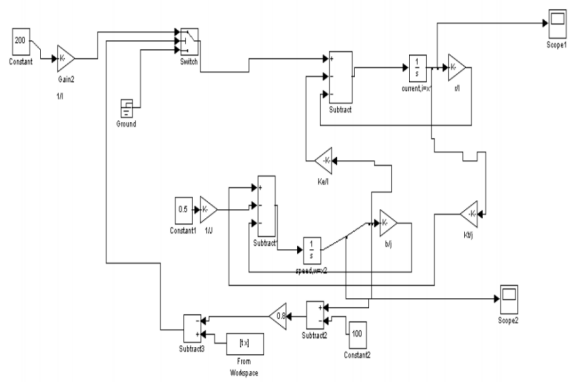

Fig. 3: Equations of the drive simulated with SIMULINK

The dynamic behavior of the DC drive can be found from the bifurcation diagram drawn with different parameters value. The bifurcation diagram with input voltage as the parameter is shown in Fig. 4. It is essential to study the occurrence of chaos due to the variation of system parameters. When bifurcation occurs, an abrupt change in the steady state behavior of the system also occurs. A bifurcation diagram represents all plots of the steady state orbits as a function of a bifurcation parameter.

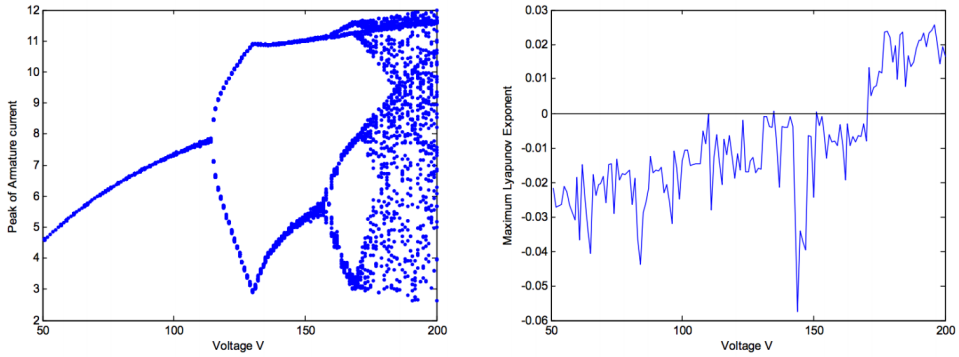

Fig. 4: Bifurcation diagram with input voltage as parameter and plot of maximum Lyapunov exponent

This shows that a period doubling route to chaos is followed. The occurrence of chaos is quantified by maximum Lyapunov exponent.

The Period-1 behavior is observed up to input voltage, 120V. Fig. 5 shows the simulated waveform of armature current for period-1 orbit at input voltage 100 V. Fig. 6 shows the time plot of speed and phase plot of armature current and speed for the same voltage. Bifurcation to different periodic orbit and chaos is observed with the increase of input voltage. The system bifurcates to period-2 after period-1. After period-2, period-4 behavior starts at a voltage of 158 V and continues up to 170 V. Period-8 behavior is observed after that. The period-8 converges to chaos at 170.5 V.

The period-2 sub harmonic waveform is shown in Fig.7. The period-2 behavior changes to period-4 after that. The period-4 behavior that occurs at 160V is shown in the Fig. 8. At input voltage of 170.5, the system shows period-8T sub harmonic (Fig.9, 10). Finally chaotic behavior of the drive is shown in Fig. 11.

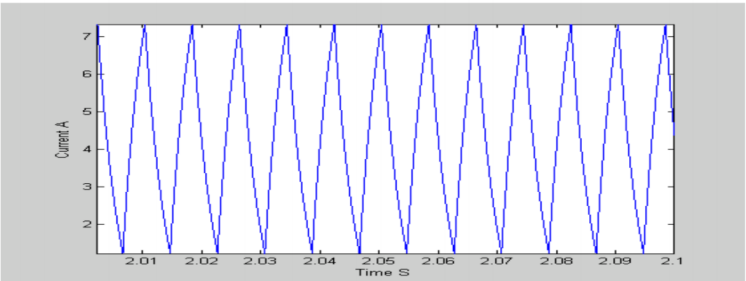

Fig. 5: Time plot of armature current showing P-1 at input voltage 100 V

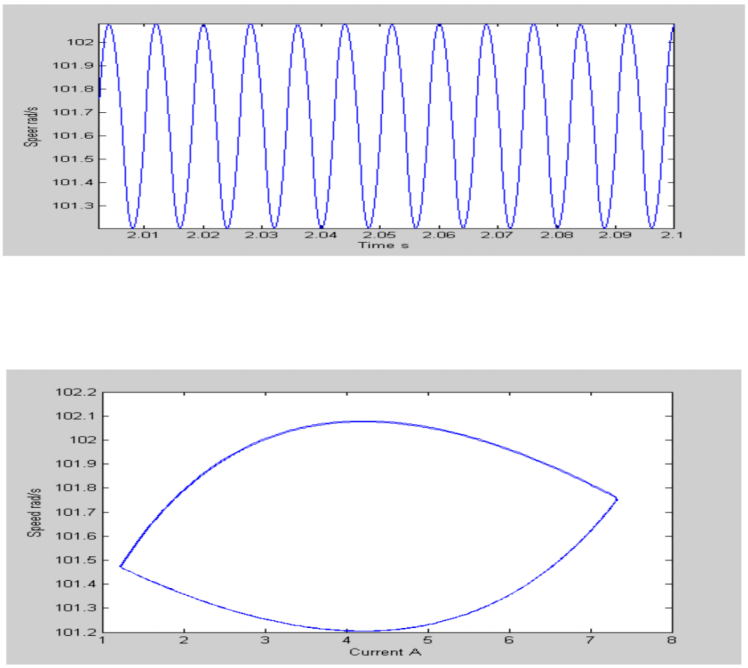

Fig. 6: (*Upper*) Time plot of speed and (*Lower*) Phase plot of armature current and speed showing P-1 at input voltage 100V

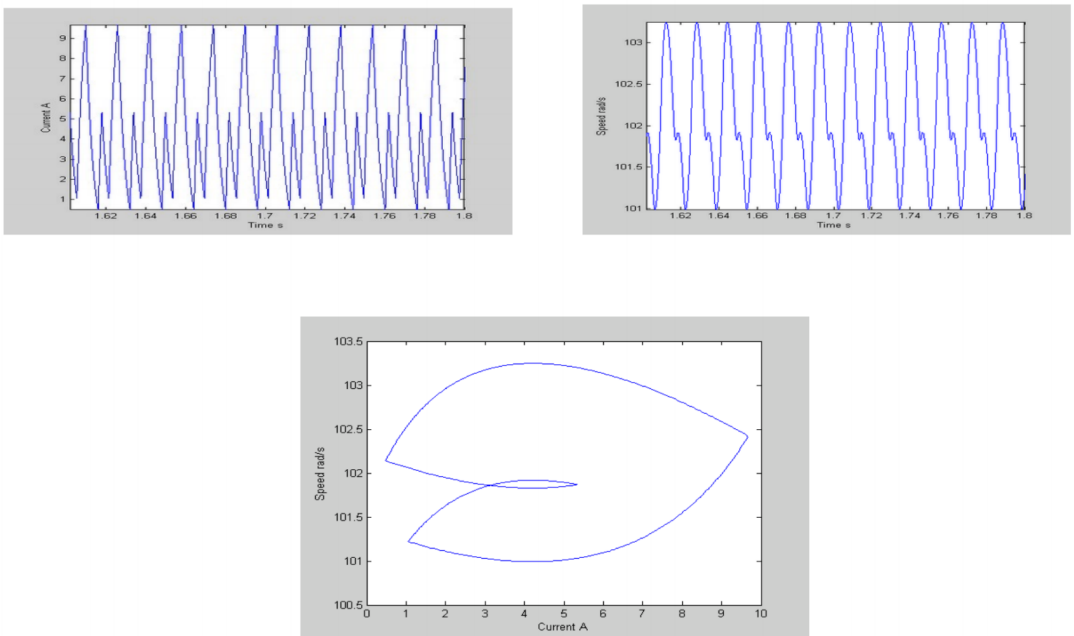

Fig. 7: Time plot of armature current, speed and phase plot showing P-2 at input voltage 150V

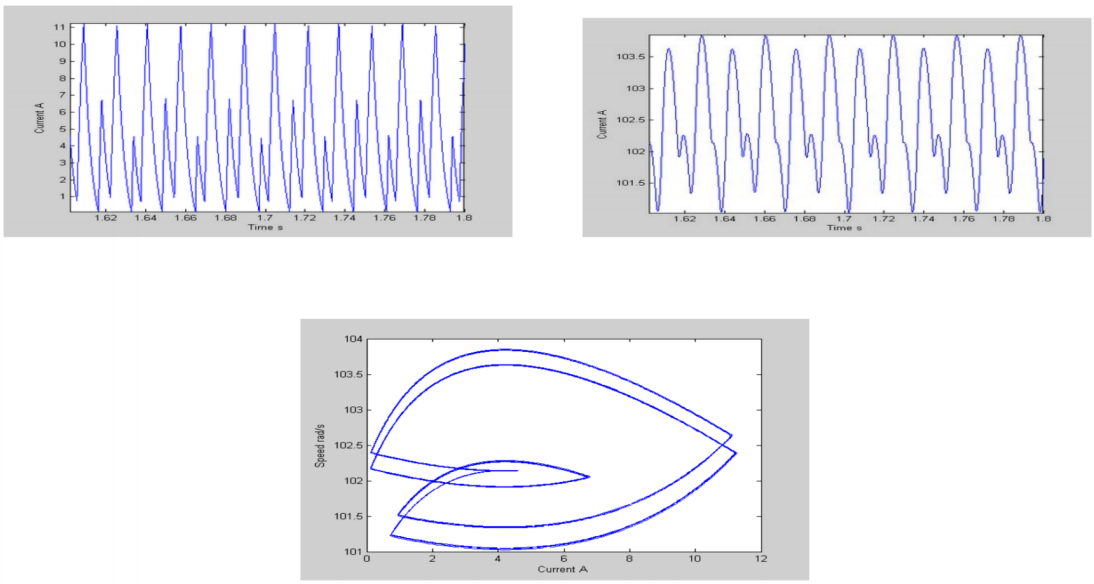

Fig. 8: Time plot of current, speed & phase plot showing P-4 at input voltage 160 V

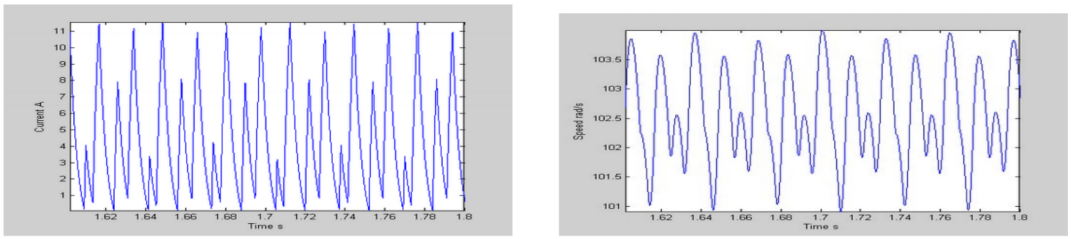

Fig. 9: Time plot of current & speed showing P-8 at input voltage 170.5 V

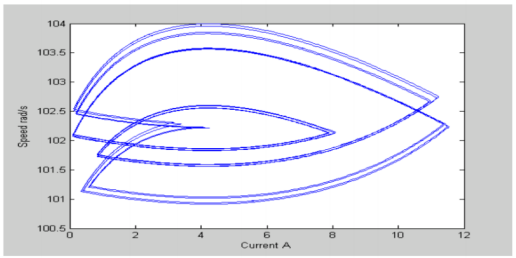

Fig. 10: Phase plot showing P-8 at input voltage 170.5 V

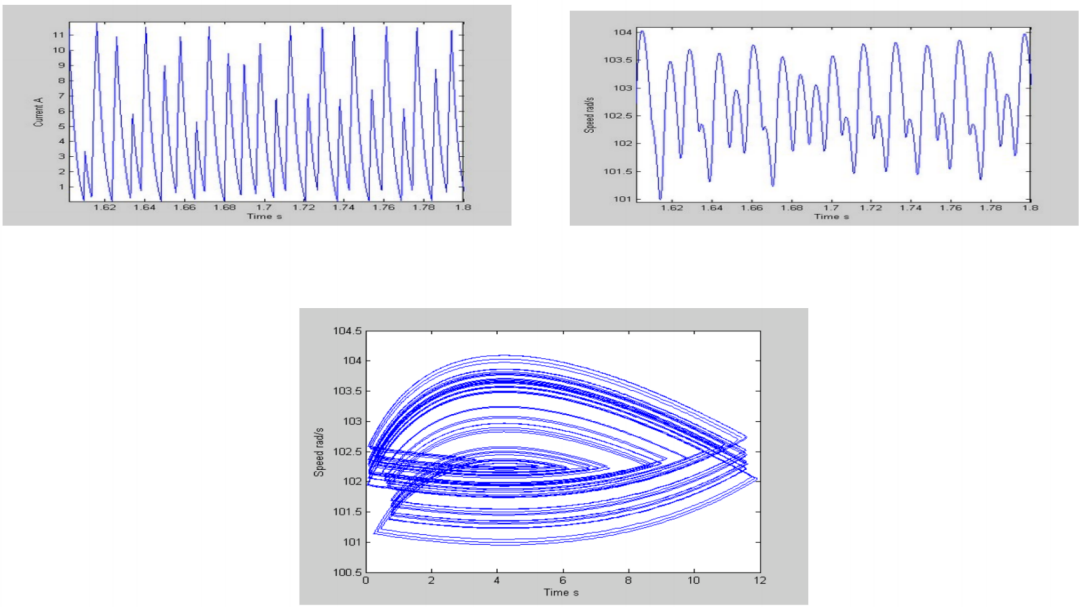

Fig. 11: Time plot of current, speed and phase plot showing chaos at input voltage 200 V

Fig. 12 shows the bifurcation diagram with gain as the parameter. The period-1 behavior is observed up to gain 0.32. The period-1 bifurcates to period-2 at 0.33. The period-2 continues up to gain 0.43. Then period-4 starts. After that the period doubling route to chaos is followed There are periodic windows in the chaotic zone. Period-1 behavior is observed at gain of 1.74. The evidence of periodic windows in the chaotic zone is evident from the plot of Lyapunov exponent. For periodic orbit Lyapunov exponent is negative and it is positive for chaos.

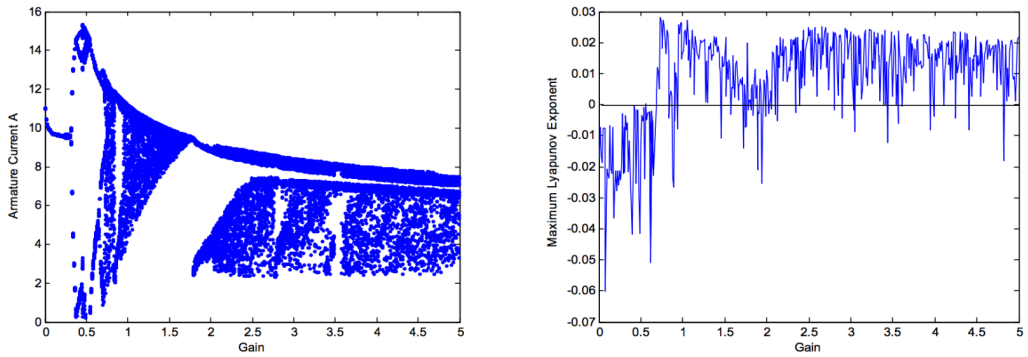

Fig.12: Bifurcation diagram with gain as parameter & plot of maximum Lyapunov exponent.

The bifurcation behavior with load torque as parameter is shown in Fig. 13. This behavior is the reverse of behaviors shown in Fig. 4 and Fig. 12. The system shows chaotic behavior at lower value of torque. With decrease of value of torque, period 1 bifurcates to period 2 and then to chaos.

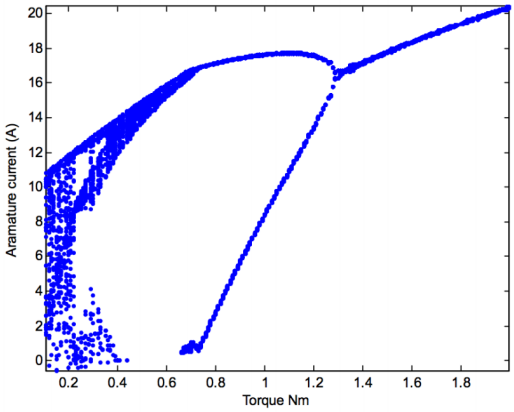

Fig.13: Bifurcation diagram with load torque as parameter

4. Stability analysis of Period-1 Orbit

We are interested in the stability of period-1 orbit of the DC drive for its normal operation. This orbit starts at a clock instant and comes back to the same state at the end of the clock period. The DC drive is not a smooth system. The equation of evolution during switch on and switch off and vice versa are smooth as shown in equation (2&3). However, at the instant of switching, the evolution becomes nonsmooth. Filippov [8] showed that in such a situation one has to additionally consider the evolution of the system across the switching event. It is known that in linear time invariant (LTI) system, the state transition matrix is given by the $\phi = e^{At}$ where A is the state matrix. The basis of the Filippov's method is to find out state transition matrix over the complete cycle including switching. The whole cycle include the switch on duration, switch off duration and switching instants. The state transition matrix that relates the evolution just after the switching event to that just before is called the saltation matrix, S and is given by

$$S = I + \frac{(f_{on} - f_{off})n^T}{n^T f_{off} + \frac{dh}{dt}}$$

where I is the identity matrix, ***h(x,t)=0*** represents the switching condition, ***n*** is the vector normal to the switching surface and $\boldsymbol{n^T}$ is its transpose, $\boldsymbol{f_{off}}$ represents the right hand side of the differential equation before switching occurred and $\mathbf{f_{on}}$ represents the right side of the differential equation after switching. From this the saltation matrix is calculated after each switching event. Since we are interested in the stability of the periodic orbit exhibited by the drive, we need to calculate the state transition matrix over the whole cycle. This matrix is called monodromy matrix. If the switch is ON at time **0** till time ***dT*** (where ***d*** is the duty cycle and ***T*** is the period) and the switch remain OFF from ***dT*** till time **T**, then the monodromy matrix is expressed as

$$\phi_{cycle}(T,0) = S_2 \times \phi_{off}(T, dT) \times S_1 \times \phi_{on}(dT, 0)$$

where S_1 is the saltation matrix related to first switching and S_2 is that related to the second switching. If the moduli of all the eigen values of the monodromy matrix, called Floquet multiplier, are less than unity, then the system will be stable.

For the drive under consideration

$$f_{on} = \begin{bmatrix} -\frac{Ra}{La}x(1)_{off} - \frac{K_E}{L}x(2)_{off} + \frac{V}{La} \\ \frac{K_T}{J}x(1)_{off} - \frac{B}{J}x(2)_{off} - \frac{T_L}{J} \end{bmatrix}$$

$$f_{off} = \begin{bmatrix} -\frac{Ra}{La}x(1)_{off} - \frac{K_E}{La}x(2)_{off} \\ \frac{K_T}{J}x(1)_{off} - \frac{B}{J}x(2)_{off} - \frac{T_L}{J} \end{bmatrix}$$

$x(1)_{off}$ and $x(2)_{off}$ represents the values of state variables (current and speed) at the instant of switch on.

$$\phi_{on} = e^{AdT}, \phi_{off} = e^{A(1-d)T}$$

$$h(x,t) = G[x(2) - \omega_{ref}] - V_L - \frac{(V_u - V_L)t}{T} = 0 \quad n = \begin{bmatrix} \frac{dh}{dx(1)} \\ \frac{dh}{dx(2)} \end{bmatrix} = \begin{bmatrix} 0 \\ G \end{bmatrix} \& \frac{dh}{dt} = -\frac{V_u - V_L}{T}$$

$$f_{on} - f_{off} = \begin{bmatrix} \frac{V}{La} \\ 0 \end{bmatrix} \& (f_{on} - f_{off})n^T = \begin{bmatrix} 0 & \frac{GV}{La} \\ 0 & 0 \end{bmatrix} \quad n^T f_{off} = G \times \frac{K_t x(1)_{off} - Bx(2)_{off} - T_l}{J}$$

Consequently, the saltation matrix for the DC drive at the switching instant (1-d) T is given by

$$S = \begin{bmatrix} 1 & \left(\frac{\frac{GV}{La}}{G\left(\frac{K_t x(1)_{off} - Bx(2)_{off} - T_l}{J} \right) - \frac{V_u - V_l}{T}} \right) \\ 0 & 1 \end{bmatrix}$$

For the given set of parameter and input voltage 100V, we obtain d= 0.4706 and

$$\phi_{on} = \begin{bmatrix} 0.3734 & -0.0108 \\ 0.3264 & 0.9942 \end{bmatrix}, \phi_{off} = \begin{bmatrix} 0.3298 & -0.01116 \\ 0.3488 & 0.9932 \end{bmatrix}$$

$$S_1 = \begin{bmatrix} 1 & -4.4283 \\ 0 & 1 \end{bmatrix}, \phi_{cycle} = m = \begin{bmatrix} -0.4574 & -1.6573 \\ -0.0498 & -0.4521 \end{bmatrix}$$

The second saltation matrix $\mathbf{S_2}$ is related the switching from the ON state to the OFF state at the end of the clock cycle turns out to be identity matrix as the falling edge of the ramp causes the **dh/dt** term to be infinity.

The values of $x(1)_{off}$ and $x(2)_{off}$ can be found out by solving state equations (3). The duty cycle, **d**, is found out by solving the equation ***h(x,t)=0.***

The eigen values of the monodromy matrix were found to be -0.7420 and -0.1675. This is expected from the bifurcation diagram (Fig. 4). All eigen values are less than unity. Hence the period-1 orbit is stable.

For some values of the supply voltage $\in$ (55,120) and gain, $\in$ (0.1, 0.4) the Floquet multipliers were computed and the results are shown in Table 1 and Table 2. The corresponding loci are shown in Fig. 14 & 15. A bifurcation is described by crossing of multiplier from the interior of the unit circle to the exterior.

Table 1:

Voltage	Floquet multipliers	Remark
55	0.2910 $\pm$j0.0.19901	Period-1 stable
100	-0.7432,-0.1672	Period-1 stable
116	-0.9209,-0.1349	Period-1 stable
120	-1.0661,-0.1165	Period -2

Table 2:

Gain	Floquet multipliers	Remark
0.1	0.0898 $\pm$j0.3409	Period-1 stable
0.2	0.2542 $\pm$j0.2442	Period-1 stable
0.32	-0.8710,-0.1427	Period-1 stable
0.38	-0.1130,-1.0992	Period -2

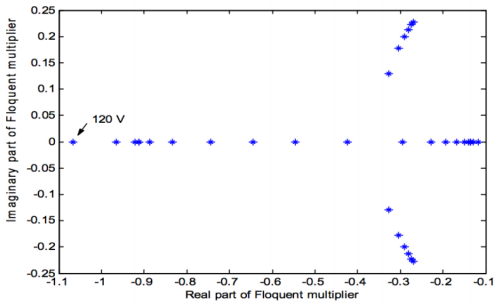

Fig. 14: Loci of Floquet multipliers for V $\in$ (55,120)

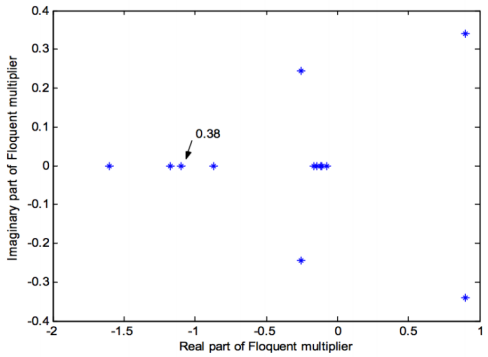

Fig.15: Loci of Floquet multipliers for gain $\in$ (0.1,0.4)

5. Conclusion

In this paper occurrence of chaos has been demonstrated by MATLAB simulation. The bifurcation diagram drawn gives the behavior of the system at different parameters. The calculation maximum Lyapunov exponent quantifies the occurrence of chaos. The stability analysis with the help of monodromy matrix and its eigen values gives the stability properties of the drive. The stability of period-1 can be greatly influenced by appropriate manipulation of the saltation matrix of the system. Based on the observation, we are able to design a controller capable of extending the parameter range for stable period-1 operation. This information is very important for the designer to design the drive system.

Acknowdgement

The authors would like to thank A.I.C.T.E for sanction of research grant under RPS to carry out the work.

REFERENCES

[1] K.T. Chau, J.H. Chen, C.C. Chan, Jenny K.H. Pong and D.T.W Chan, *Proceeding of IEEE power electronics and drive systems*, Singapore (1997) 473.

[2] K. Chakrabarty, U. Kar and S. Kundu, "Chaotic behavior in a DC series drive", *Proceeding of National Power Electronic Conference-2010*, IIT Roorkee, 8-10 June 2010.

[3] K. Chakrabarty, U. Kar and S. Kundu, ``Chaotic behavior in a speed controlled DC series drive", *Proceeding of National system Conference-2010*, NITK, 10-12 December 2010.

[4] K. Chakrabarty, U. Kar and S. Kundu, ``Chaotiozation of DC Series motor for industrial mixing", *Proceeding of National system Conference-2010*, NITK 10-12 December 2010.

[5] K. Chakrabarty, U. Kar and S. Kundu, ``Chaos in current controlled DC Series drive", *Proceeding of National Conference on Advances In Energy Conversion Technologies*, MIT 3-5 February 2011.

[6] K. Chakrabarty, U. Kar and S. Kundu,``Bifurcation behavior and Co-existing attractor of PWM controlled DC drives", *Proceeding of IEEE (INDICON-2011) Conference-2011*, 17-18 December 2011.

[7] A.F. Filippov, *Differential Equations with discontinuous right hand sides*, Kluwer, Dordrecht, The Natherlands (1988).

[8] R.I. Leine and H. Nijmeijer, *Dynamics and bifurcation of non-smooth mechanical systems*, Springer-Verlog, Berlin, Germany (2004).

[9] D. Giaouris, S. Banerjee, B. Zahawi and V. Pickert, "Stability analysis of the continuous conduction mode Buck converter via Filippov's method", IEEE Transaction on circuits and systems I Fundamental theory and application, **55** (2008) 1084.

[10] N.C. Okafor, D. Giaouris, B. Zahawi and S. Banerjee, "Analysis of fast–scale instability in DC drives with full-bridge converter using Filippov's method'', 5th IET International Conference on Power Electronics, Machines and Drives (PEMD 2010), **DOI:** 10.1049/cp.2010.0191.

[11] C. Morel, D. Petreus and A. Rusu, Advances in Electrical and Computer Engineering, **11** (2011) 93.

Scientific Voyage
Vol. 1, No. 1,
Page 13-20 (2020)

SCIENTIFIC VOYAGE
ISSN: 2395-5546

ISSN: 2395-5546

Calcination Characteristics of Limestone in relation with the reactivity of Quick Lime

Tapas Kumar Bhattacharya[1] and Kaushik Maity[2]

[1]*Department of Ceramic Technology,*
Government College of Engineering & Ceramic Technology, Kolkata - 700010, WB, India
E-mail: tkb_ceramics@yahoo.co.in

[2]*Department of Ceramic Technology,*
Government College of Engineering & Ceramic Technology, Kolkata - 700010, WB, India
E-mail: kaushikjordan24@gmail.com

Abstract: The present work is focused on the calcination characteristics of limestone at the temperature range of 750^{0}C to 900^{0}C with one hour soaking followed by the derived quick lime is fully hydrated to slaked lime. The carbonate derived and hydroxide derived nascent lime differ reactivity in a significant extent. The carbonate derived lime in single stage process is less susceptible to hydration than hydroxide derived lime in double stage process. Limestone when calcined at 950^{0}C, the derived lime shows 1.2 percent weight gain but hydroxide when calcined at 570^{0}C, the derived lime shows hydration affinity of 5.2 percent weight gain. The surface area of born lime decreases with Calcination temperature of both carbonate and hydroxide. The high reactivity of hydroxide derived lime is due to higher surface area of newly born CaO than from carbonate as well as hydroxide derived lime form at comparatively lower temperature than carbonate. The hydration affinity increases with increasing surface area.

Keywords: Calcination; Limestone; Quick Lime

1. Introduction

Lime in the various form as quicklime obtained by light calcination of limestone and slaked lime obtained by hydration of calcined product of limestone. It is an attractive material and has extensively industrial application as a binder for the production of hydraulic mortars, plasters, filler in plastic, manufacture of cement as well as fluxing material in metallurgical process to remove the gangue present in naturally occurring ores [1-4]. The decomposition of $CaCO_3$ is highly endothermic process with ΔH = +178 kj/mole and the rate of calcination increases at higher temperatures, as well as at higher partial pressures of carbon dioxide and steam vapour [5]. The reactivity of quick lime depends on various factors like characteristics of the limestone, calcination temperature, pressure acquired in kilns, rate of calcination, fuel quality and presence of associated impurities like SiO_2 , Al_2O_3, Fe_2O_3 in limestone [6,7].

The presence of impurities in limestone increases the sintering rate which changes the pore shape, increase pore shrinkage and grain size that CaO particles undergo during heating. Densification increases at higher temperatures, as well as at higher partial pressures of carbon dioxide and steam vapour [8]. The reactivity of lime produce by calcination of limestone differ mainly due to surface area of nascent CaO. Beruto

et al. [9] found that coarser grain limestone resulted in surface areas of CaO only 2 to 5 m^2/g when calcined in a rotary kiln at 980°C whereas Chan et al. [10] attained a surface area of 24.6 m^2/g by calcining limestone particles in a TGA at 745°C. The surface area of born CaO by the calcination of limestone depends on so many factors like the characteristics of the limestone, calcination temperature, pressure acquired inside the kilns, rate of calcination, and fuel quality [11,12]. Lime has also been used as a hydraulic binder for the production of mortars, plasters and a pure binder to get aerial mortar or mixed with natural or artificial pozzolana for the manufacture of hydraulic mortars [13].

The present study is focused on the nature and reactivity of lime derived directly by calcination of limestone or limestone derived slaked lime. The carbonate derived or hydroxide derived lime and their reactivity towards hydration in relation with calcination characteristics of limestone is also studied in this investigation.

2. Experimental

2.1 Materials

The purer variety limestone sample from Madhyapradesh region of India was selected as a basic carbonate source in this study. 1gm. powder limestone sample of -300 mesh was first dissolved in 1:1 HCl solution followed by makeup volume to 250 ml. The chemical analysis was carried out from this stock solution as per standard ASTM C25 – 19 and the analysis report was expressed in terms of oxide basis.

The reactivity of lime was varied by changing the calcinations of parent materials. The carbonate derived lime was prepared by calcinations of limestone at about 900^0C followed by 1hour soaking but hydroxide derived lime was prepared by calcinations of limestone first at about 900^0C followed by slaking of oxide by large excess water to form calcium hydroxide. The hydroxide powder was then calcined to oxide powder.

2.2 Characterisation of Materials

The phase analysis of limestone was characterised was carried out by X-ray diffraction techniques using a Rigaku (Japan) Ultimal III diffractometer with monochromatic Cu-Kα radiation (1.54059Å) at 40 kV and 30 mA. The scanning span (2θ) is ranged from 10° to 80° at a scanning speed of 1°/min. The surface morphology of limestone was characterised by thin section optical microscopy techniques. The decomposition behaviour of limestone was characterised by DTA techniques at the heating rate of 10^0C/min by using α-alumina as an inert material. The hydration of different reactive lime was carried out by taking weight gain of CaO powder taken in a Petridis at 70^0C and 90 percent relative humidity for 2 hours in a steam humidity cabinet. After hydration the Petridis was dried at 110^0C in an air oven to remove the adhering moisture from the powder surface. The percent weight gain was calculated on the basis of initial weight of CaO powder.

3. Results and Discussion

The natural carbonate material limestone from Madhyapradesh region of India, selected in this study is relatively pure with a very low amount of impurities around 2 weight percent. The chemical analysis of raw limestone on oxide basis is shown in Table 1.

Table 1: Chemical Analysis of raw limestone

SiO_2	Al_2O_3	Fe_2O_3	CaO	MgO	Na_2O	K_2O	LOI
1.48	0.20	0.11	54.56	Traces	0.11	0.33	42.888

X-ray diffraction pattern of limestone in Fig. 1 shows that diffraction peaks corresponding to calcite only at (012), (104), (110), (113), (202), (108) and (116) and no aragonite and vaterite was present. These results supported by other researchers [4,6,9].

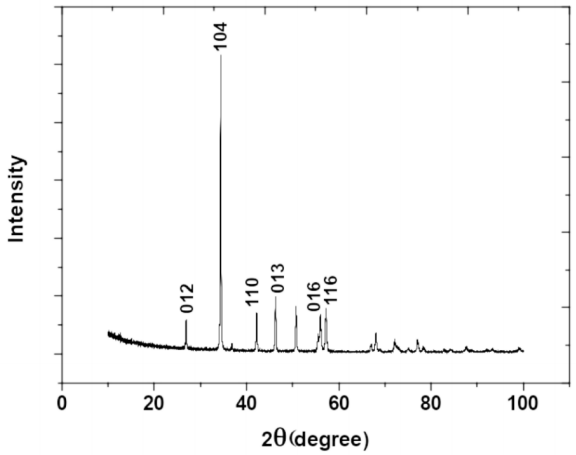

Fig. 1: X-ray diffraction pattern of limestone

The surface morphology of raw limestone rock in Fig. 2 shows that it consist of rounded to subrounded calcite grain with a granular texture contact situredly with uniaxially negative. The grains are mostly colourless in plane polarised light but in crossed polarised light it shows higher order interference colour. One set of parallel cleavage and rhombic cleavage are clearly visible in some grains [10,12]. The average grain size was 125 µm.

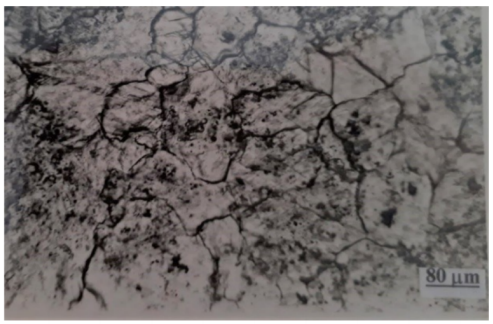

Fig. 2: The surface morphology of raw limestone rock

The differential thermal analysis of limestone is shown in Fig. 3. There is a highest endothermic peak at around 916^{0}C for limestone which is very much comparable with the literature, the dissociation occur at 825^{0}C to as high 923^{0}C depending upon the nature, quality and largely on heating rate (14-17). The hydroxide derived from limestone decomposes earlier at 515^{0}C than carbonate.

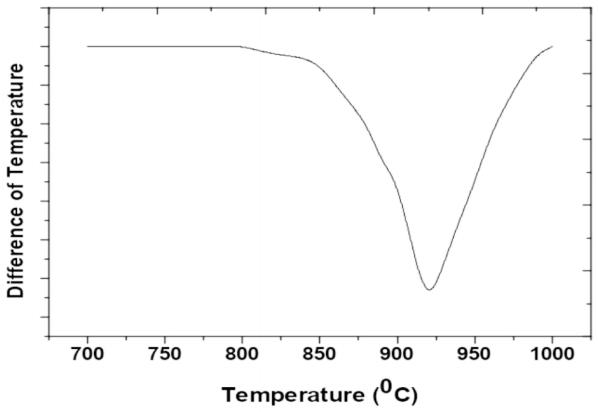

Fig. 3: The differential thermal analysis of limestone

The surface area of nascent lime derived from carbonate and hydroxide in relation with calcination temperature is shown in Figs. 4(a) & 4(b).

The surface area gradually decreases with increasing calcination temperature both in carbonate and hydroxide derived lime. The hydroxide derived lime shows higher surface area than carbonate derived lime. This is due to hydroxide decomposes comparatively lower temperature than carbonate which create more immune and less reactive surface of carbonate derived lime [17-19].

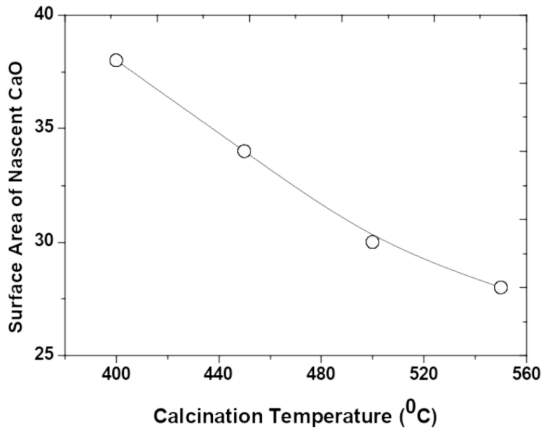

Fig. 4(a): The surface area of nascent lime derived from hydroxide in relation with calcination temperature

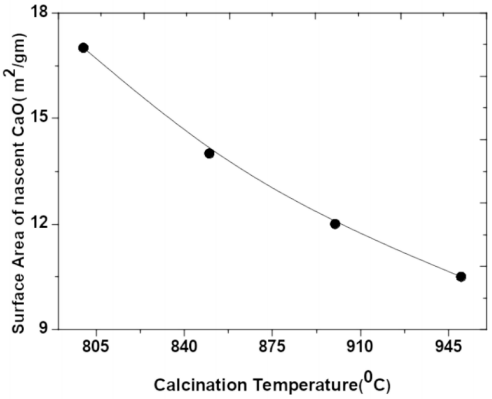

Fig. 4(b): The surface area of nascent lime derived from carbonate in relation with calcination temperature

Hydration is the chemical combination of CaO with water to form $Ca(OH)_2$, an importance characteristics of lime. The structural openness and thermodynamics instability causes the lime to hydrate even when CaO comes in contact with atmospheric moisture. The hydration mechanism is believed to occur in two stages (i) reversibly adsorbed water on the surface of CaO particle to form $Ca(OH)_2$ which initially cover the oxide surface and (ii) secondary adsorbed water diffuse through hydroxide layer subsequently hydrate oxide grains. This diffusion is much slower process which controls the rate of hydration of CaO [20,21]. The hydration affinity of CaO depends on the reactivity of lime.

Figs. 5 & 6 showed that Percent weight gain of CaO decreases with calcination temperature of parent carbonate or hydroxide. This is because with increasing calcination temperature the born lime becomes more immune to hydrate. Dehydration of hydroxide occur at lower temperature than decarbonation of carbonate and hydroxide derived oxide has an enormous surface area and free energy than those of carbonate derived oxide which causes the more reactivity of hydroxide derived lime [16].

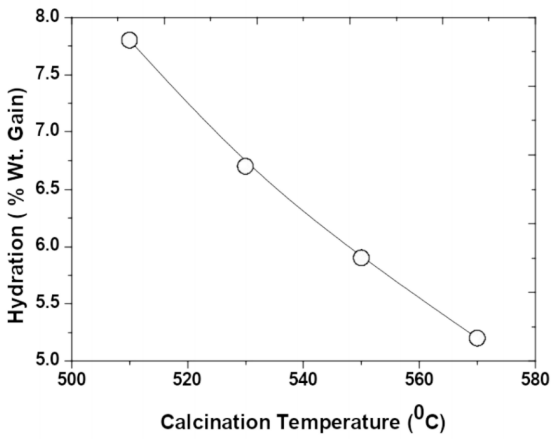

Fig. 5: Hydration (% Wt. Gain) vs. Calcination Temperature of lime derived from hydroxide

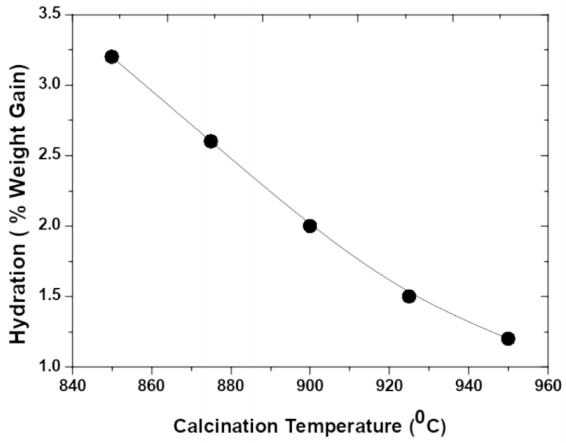

Fig. 6: Hydration (% Wt. Gain) vs. Calcination Temperature of lime derived from Carbonate

Fig. 7 showed that hydration of CaO is a strong function of its surface area. With increasing surface area of CaO the percent weight gain increases due to enhancement of rate of chemisorptions of water on the grain boundary surface. More the surface area diffusion of water is more causes more hydration [19-21].

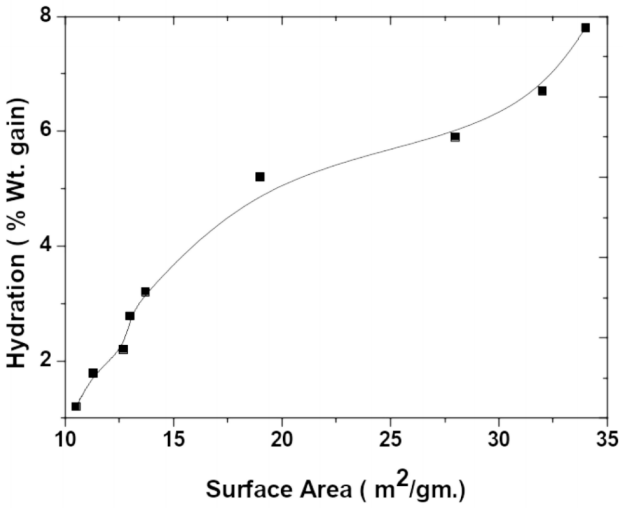

Fig. 7: Hydration (% Wt. Gain) vs. Surface area of CaO

4. Conclusion

The reactivity of born lime from limestone towards hydration is less than hydroxide derived lime due to high surface area of born CaO from hydroxide. Hydration gain of born CaO decreases with calcinations temperature of both carbonate and hydroxide. The chemisorptions of hydration process depends mainly on the

surface area of born CaO. Hydration gain decreases with surface area due to enhancement of chemisorptions which increases hydration gain.

REFERENCE

[1] R. Malinowsky and Y. Grafinkel, *Concr. Int*., **62** (1991) 13.

[2] M. Wingate, *Inter. Tech. Pub*., London (1985).

[3] D. Beruto, L. Barco and A.W. Searcy, *J. Am. Ceram. Soc*., **66** (1983) 893.

[4] R.H. Borgwardt et al., *Indust. Engg. Chem. Res*., **26** (1987) 1993.

[5] E.K. Powelland and A.W. Searcy *J. Am. Ceram. Soc*., **65** (1982) 219.

[6] L. Yang and W. Zhang, *Inorg. Chem. Ind*., **44** (2012) 16.

[7] R.M. German and Z.A. Munir , *J. Am. Ceram. Soc*., **59** (1976) 379.

[8] L. Barco, et al. (1980) *J. Am. Ceram. Soc*., **63** (1980) 439.

[9] R.H. Borgwardt, *Chem. Engg. Sc*. **44** (1989) 53.

[10] R.K. Chan, K.S Murthi and D. Harrison. *J. Chem*., **48** (1970) 2972.

[11] R. Pacciani et al., *Energy Fuels,* **21** (2007) 2072.

[12] R.H. Borgwardt, *AIChE J.,* **31** (1985) 103.

[13] P. Sun et al., *AIChE J.,* **53** (2007) 2432.

[14] P.J. Anderson et al., *Proc. Br. Ceram. Soc*, **3** (1965) 33.

[15] V. Manovic et al., *Energy Fuels,* **22** (2008) 3258.

[16] R.H. Borgwardt, *Indust. Engg. Chem. Res*., **28** (1989) 493.

[17] D. Beruto and A.W. Searcy, *J. Chem. Soc. Faraday Trans*., **170** (1974) 2145.

[18] S.J. Bortz et al., ``Precalcination and Its Effect on Sorbent Utilization during Upper Furnace Injection,'' in Proceedings: 1986 Joint EPRI/EPA Symposium on Dry SO2 and Simultaneous SO2/N0x Technologies, Volume 1, EPRI CS4966, December 1986.

[19] C.R. Milne and G.D. Silcox, *Indust. Engg. Chem. Res.,* **29** (1990) 139.

[20] D. Beruto et al., *J. Amer. Cer. Soc*, **67** (1984) 512.

[21] W. Zhang, C. Chun-Bao and D. Fu-Jun, *Bul. Chin. Ceram. Soc*., **29** (2010) 926.

Scientific Voyage
Vol. 1, No. 1,
Page 21-25 (2020)

SCIENTIFIC VOYAGE
ISSN: 2395-5546

ISSN: 2395-5546

Bose-Einstein Condensation in a Uniformly Accelerated Frame

Sanchita Das[1] and Somenath Chakraborty[2]
[1] *Department of Physics, Visva-Bharati, Santiniketan 731235, West Bengal, India; E-mail: sanchita.vbphys@gmail.com*
[2] *Department of Physics, Visva-Bharati, Santiniketan 731235, West Bengal, India; E-mail: somenath.chakrabarty@visva-bharati.ac.in*

In this article we have investigated the possibility of Bose-Einstein Condensation (BEC) in a frame undergoing uniform acceleration or in other wards, in Rindler space associated with the uniformly accelerated frame. We have followed a very simple conventional technique generally used in text book level studies. It has been observed that the critical temperature for BEC increases with the increase in magnitude of acceleration of the frame. Typically the critical temperature in an accelerated frame is of the order of the Unruh temperature. Hence we have concluded that the increase in the magnitude of acceleration of the frame facilitates the formation of condensed phase

Keywords: Bose condensation; Rindler space; Uniformly accelerated frame; Principle of equivalence

1. Introduction

Since bosons do not obey Pauli exclusion principle, the total wave function for a system consisting of a number of bosons is symmetric in nature. Then at low temperature, less than a typical value known as the critical temperature for BEC, a substantial number of bosons will go to the ground state energy level or zero energy level [1,2]. In a certain sense, the BEC is akin to the familiar process of liquid-vapor phase transition. Conceptually, however, the two process are very different. Unlike the liquid-vapor transition, which occured in configuration space, the BEC takes place in momentum space-described as a condensation in momentum space [3]. However with the critical examination of the equation of states of non-BEC and BEC phases shows the first order nature of the phase transition [3]. The term momentum space condensation is the thermodynamic manifestation that the transition to BEC state occurs only because of the symmetric nature of the wave function and not because of any inter particle interaction [4]. This is the very reason why it takes so many years to verify it experimentally. Although it has been predicted long ago [1,2], only in the year 1995 the phenomenon was experimentally verified [5,6]. The advancement of technology, in particular,the progress in low temperature physics, including the associated cryogenic technology helps a lot to conduct this experiment. Two experimental condensed matter physicist, Eric Cornell and Carl Wieman were awarded Nobel prize in the year 2001 to verify the formation of BEC. They have used a few hundreds of Rb^{87} atoms, which are bosons. These atomic bosons were trapped in a harmonic potential [3]. They have obtained BEC at around 170 Nano K.

Let us now introduce in brief the concept of Rindler space. It is associated with a frame undergoing uniform accelerated motion with respect to some inertial frame [7–10]. The Rindler space can very easily be shown to be flat in nature (curvature tensors are zero in this case). Therefore one can say that the Rindler space

is a kind of flat Minkowski space where the uniform velocity of the moving frame (inertial in nature) is replaced by uniform acceleration (non inertial in nature). Now from the principle of equivalence a frame undergoing acceleration in absence of gravity is equivalent to a frame at rest in presence of a gravitational field of which the strength of gravitational field is exactly equal to the magnitude of the acceleration [10]. Therefore in the present situation it is equivalent to say that we are going to study BEC in a rest frame but in presence of a strong uniform background gravitational field.

Now it can very easily be shown that in the Rindler space the Hamiltonian of a particle of rest mass m_0 is given by [11–15] (see also [16–18])

$$H = \left(1 + \frac{\alpha x}{c^2}\right)\left(p^2c^2 + m_0^2c^4\right)^{1/2}, \tag{1}$$

where it is assumed that the frame is undergoing accelerated motion along x-axis, which is of course arbitrary in nature, indicates that the space spanned on $x - y$ plane is isotropic. The acceleration or the gravitational field α is constant within a length parameter x_0 (say). Then in our formalism we replace x in the above expression by x_0. For the sake of convenience one can use without the loss of generality the non-relativistic approximation of the above equation, given by

$$H = \left(1 + \frac{\alpha x}{c^2}\right)\left(\frac{p^2}{2m_0} + m_0c^2\right). \tag{2}$$

At this point we should mention that in quantum mechanical picture the above Hamiltonian H (both in relativistic and non relativistic scenario) is non-Hermitian. But is PT symmetric in nature, where P is the parity operator and T is the time reversal operator [19]. As a consequence the eigen spectrum of H is real in nature.

2. Basic Formalism

The effect of background gravitational field on the energy eigen value has come through the Rindler Hamiltonian H containing the term α. We have noticed that even in quantum mechanical studies in Rindler space the strong gravitational field affects the binding of the particles [17]. Now below the critical temperature T_c for the transition to BEC one can write

$$n = n_{p\neq 0} + n_{p=0}, \tag{3}$$

where n is the total number of bosons per unit volume and on the right hand side, the first term is the total number of normal bosons per unit volume and the second term is the corresponding quantity per unit volume in the BEC phase. In the usual case

$$n = \frac{1}{\lambda^3} g_{3/2}(z) + \frac{z}{1-z} \times \frac{1}{V}, \tag{4}$$

where $\lambda = h/(2\pi mkT)^{1/2}$, the thermal de-Broglie wavelength, z is the fugacity, $V = S_{yz}dx$ the volume of a small cylinder of cross sectional area S_{xy} with the corresponding length element dx and the function $g_{3/2}(z)$ is given by the infinite series

$$g_{3/2}(z) = \sum_{l=1}^{\infty} \frac{z^l}{l^{3/2}}. \tag{5}$$

Here the volume element V is completely arbitrary in which the field α is constant, however, we are not using this expression explicitly in our analysis. Therefore the arbitrariness is not going to affect our conclusion. The function $g_{3/2}(z)$ is a monotonically increasing function of z and is bounded within the domain $0 \leq z \leq 1$. At $z = 1$, $g_{3/2}(1) = 2.612$, beyond which it diverges to $+\infty$. Therefore at $T = T_c$, the critical condition [3]

$$n = \frac{1}{\lambda^3} g_{3/2}, \tag{6}$$

gives the critical temperature for BEC. Obviously at T_c, the chemical potential μ for the Bose particles is zero or in the relativistic scenario is m_0c^2, the rest mass energy. Therefore it is also quite clear that in the Rindler space, the value of μ and T_c will be completely different from that of the usual scenario. In Rindler space at $T = T_c^{(\alpha)}$ (say), where $T_c^{(\alpha)}$ is the modified critical temperature in the Rindler space and

$$\mu = \left(1 + \frac{\alpha x_0}{c^2}\right) m_0c^2 = u(\alpha) m_0c^2, \tag{7}$$

is the modified form of chemical potential when the system is under going an uniform acceleration α. Obviously, the value of the chemical potential is large enough in the Rindler space if the magnitude of the acceleration is also quite high [14]. Of course here also one has to consider $z = 1$ and then the total number of particles per unit volume is given by

$$n = \frac{1}{u^{3/2}\lambda_\alpha^3} g_{3/2}, \tag{8}$$

where $u = \left(1 + \frac{\alpha x_0}{c^2}\right)$ and λ_α is the thermal de Broglie wavelength in the Rindler space. It is quite obvious that we get back the usual solution if $\alpha = 0$, i.e., in the inertial frame or $\alpha x_0/c^2 \ll 1$. Since n is fixed (there is also no change in volume), we have from Eq. (8) (see Eq. (41) of [14])

$$T_c^{(\alpha)} = u(\alpha) T_c = \left(1 + \frac{\alpha x_0}{c^2}\right) T_c. \tag{9}$$

This is the mathematical relation connecting the critical temperatures for BEC in the two different physical scenarios.Therefore in our simplified picture, the critical temperature for BEC transition will be quite high if the quantity $\alpha x_0/c^2 \gg 1$. Which may happen because of the large enough value of α, the strength of back ground gravitational field. Assuming a typical value $x_0 = 1KM = 10^5 cm$ and $T_c = 10^{-7}$K, We have

$$T_c^{(\alpha)} \approx \left(10^{-7} + 10^{-23}\alpha\right) K, \tag{10}$$

where the uniform acceleration of the frame is expressed in the unit $\mathrm{cm/s^2}$. Therefore to affect T_c, the minimum value of uniform acceleration or the constant gravitational field must be $\approx 10^{16} cm/s^2$ and then only, the second part on the right hand side of Eq. (10) will be of the same order of magnitude as that of the first term. Let us now compare the second term with the well known Unruh temperature [20,21], given by

$$T_U = \frac{\hbar \alpha}{2\pi c k_B}. \tag{11}$$

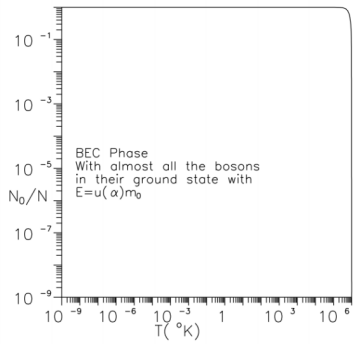

Fig. 1 Phase diagram for BEC in Rindler space (an illustration only).

The Unruh effect is associated with the quantum mechanical interaction between an accelerated observer and the inertial vacuum. Since the accelerated observer carries so much extra energy that it can transfer some of it to the inertial vacuum at the time of interaction and as a result the inertial vacuum will no longer remain vacuum. The inertial vacuum will be excited and emits radiations and particles. One can say that the vacuum state will become warmer to the accelerated observer. However, it will remain vacuum to an inertial observer at rest or in motion with uniform velocity. The expression for Unruh temperature is [20, 21]

$$T_U = \frac{\hbar\alpha}{2\pi c k_B} = 4 \times 10^{-23}\alpha/[cm/s^2][K]. \tag{12}$$

Therefore the second term on the right hand side of eqn.(10) is $\approx T_U$. Hence we may write

$$T_c^{\alpha} = T_c + T_U. \tag{13}$$

If $T_U \gg T_c$, we can conclude that the critical temperature $T_c^{(\alpha)}$ for BEC transition, in Rindler space is $\approx T_U$ [22]. Therefore we may conclude that in our simplified picture the uniform acceleration of the moving frame containing the Bose gas, the critical temperature for BEC can be quite high when observed from an inertial frame. It is shown in [22] that there exist a critical acceleration above which there is no BEC whereas it begins to appear in the accelerating frame when the acceleration is gradually decrease. We have noticed that in our formalism the chemical potential increases monotonically with the increase in the uniform acceleration of the moving frame. Which is consistent with the result obtained in [22]. In [23] the authors have obtained negative thermal-like correction associated with acceleration of the frame. They have used the thermo-field dynamics and the effect of uniform acceleration of the moving frame and gave an explanation for this negative sign and shown the increase in the fractional abundance of condensed phase with larger acceleration. Indirectly speaking our formalism is also consistent with the work presented in [23].

3. Conclusion

In our model the critical temperature $T_c^{(\alpha)} \approx T_U$. Therefore if the temperature of the Bose system in the uniformly accelerated frame is decreased continuously,

i.e., T becomes more and more less than the corresponding critical temperature, then it is quite possible that almost all the bosons will go to the condensed phase much before absolute zero temperature. To illustrate graphically, in Fig.(1) we have plotted N_0/N against T using the expression

$$\frac{N_0}{N} = 1 - \frac{T^3}{{T_c^{(\alpha)}}^3}.$$

We have considered just for the sake of illustration $T_c^{(\alpha)} = 10^{7^o}\text{K}$, the core temperature of sun and vary T ($\leq T_c^{(\alpha)}$) from 10^{-7^o}K, the approximate value of the critical temperature for BEC in the laboratory to $T_c^{(\alpha)}$, the critical temperature for BEC in the Rindler space with the value of acceleration $\alpha \sim 10^{30}\text{cm/s}^2$, which is also the corresponding Unruh temperature. However, this value of the critical temperature for BEC has very little significance as the Unruh temperature. At this temperature, there is no breaking of any kind of symmetry or particle production at the core of sun. The critical temperature for BEC in the accelerated frame must therefore be several order more than 10^7K. Further, it is quite obvious from the nature of the curve that all the bosons go to their ground state $u(\alpha)m_0$ much before $T = 0$. Therefore we may conclude that the increase in the magnitude of uniform acceleration of the frame or equivalently, the strength of constant gravitational field of the rest frame facilitates the BEC process. At the end of this article we are proposing to compare our phase diagram with the standard BEC phase digram from a standard text book on Statistical Mechanics [3].

References

1. S.N. Bose, *Z. Phys* **26** (1924) 178.
2. A. Einstein, *Sitzungsberichte (Berlin)* **1** (1925) 3-14. (see also http://www.physik.uni-oldenburg.de/condmat/TeachingSP/SP.html)
3. *Bose-Einstein condensation*, C.J. Pethick and H. Smith, Cambridge Univ. Press (2002)
4. K. Huang, *Statistical Mechanics*, John Wiley and Sons, New York (1987)
5. M.H. Anderson, J.R. Ensher, M.R. Mathews, C.E. Wieman and E.A. Cornell, *Science* **269** (1995) 198
6. K.B. Davis, M.O. Mewes, M.R. Andrews, N.J. van Druten, D.S. Durfee, D.M. Kurn and W. Ketterle, *Phys. Rev. Lett.* **75** (1995) 3969
7. L.D. Landau and E.M. Lifshitz, *The Classical Theory of Fields*, Butterworth-Heimenann, Oxford (1975)
8. N.D. Birrell and P.C.W. Davies, *Quantum Field Theory in Curved Space*, Cambridge University Press, Cambridge (1982)
9. C.W. Misner, K.S. Thorne and J.A. Wheeler, *Gravitation*, W.H. freeman and Company, New York (1972)
10. W. Rindler, *Essential Relativity*, Springer-Verlag, New York (1977)
11. G.F. Torres del Castillo and C.L. Perez Sanchez, *Revista Mexican De Fisika* **52** (2006) 70
12. M. Socolovsky, *Annales de la Foundation Louis de Broglie* **39** (2004) 1
13. C.G. Huang and J.R. Sun, arXiv:gr-qc/0701078.
14. D.J. Louis-Martinez, *Class. Quantum Grav.* **28** (2011) 036004
15. D. Percoco and V.M. Villaba, *Class. Quantum Grav.* **9** (1992) 307
16. S. De, S. Ghosh and S. Chakrabarty, *Mod. Phys. Lett. A* **30** (2015) 1550182
17. S. Mitra and S. Chakrabarty, *Euro. Phys. Jour. Plus* **71** (2017) 5
18. S. Das, S. Ghosh and S. Chakrabarty, *Mod. Phys. Lett.* **32** (2017) 1750180
19. C.M. Bender, S. Boettcher and P. Meisinger, *J. Math. Phys.* **40** (1999) 2201
20. W.G. Unruh, *Phys. Rev. D* **14** (1976) 4
21. W.G. Unruh, *Phys. Rev. D* **14** (1976) 870
22. Shingo Takeuchi, *Phys. Lett. B* **750** (2015) 209
23. S. Benic and K. Fukushima, arxiv:1503.05790v3 [hep-th].

Scientific Voyage
Vol. 1, No. 1,
Page 26-38 (2020)

SCIENTIFIC VOYAGE
ISSN: 2395-5546

ISSN: 2395-5546

Plane symmetric cosmological models

A.K. Yadav[1], A.T. Ali[2], Saibal Ray[3], Farook Rahaman[4] and Arkapriya Mallick[4]

[1] *Department of Physics, United College of Engineering and Research, Greater Noida 201306, India; E-mail: abanilyadav@yahoo.co.in*

[2] *Department of Mathematics, King Abdul Aziz University, PO Box 80203, Jeddah 21589, Saudi Arabia & Department of Mathematics, Faculty of Science, Al-Azhar University, Nasr city, 11884, Cairo, Egyp; E-mail: atali71@yahoo.com*

[3] *Department of Physics, Government College of Engineering and Ceramic Technology, Kolkata 700010, West Bengal, India; E-mail: saibal@associates.iucaa.in*

[4] *Department of Mathematics, Jadavpur University, Kolkata 700032, West Bengal, India; E-mail: rahaman@associates.iucaa.in*

[4] *Department of Mathematics, Jadavpur University, Kolkata 700032, West Bengal, India; E-mail: arkopriyamallick@gmail.com*

Abstract: In the present work, we execute the Lie symmetry analysis on the Einstein-Maxwell field equations in the plane symmetric spacetime. Under the background of the plane symmetric space-time we compute the Lie point symmetries, perform the similarity reductions and obtain exact solutions in connection to the evolutionary scenario of the universe. The special feature of the study is that it deals with the electromagnetic energy of the inhomogeneous universe through the non-vanishing component of electromagnetic field tensor F_{12} and assumes that the free gravitational field is of Petrov type-II non-degenerate. We have found that the electromagnetic field tensor is positive and increasing function of time. To validate the solution set, we examine with detailed discussions several physical as well as geometrical features of a specific sub-case of the model.

Keywords: Cosmological model; Einstein-Maxwell space-time; Lie point symmetry; Petrov type-II

1. Introduction

The Friedman-Robertson-Walker (FRW) [1] cosmological model describes a universe that configures the smoothness of the cosmic spacetime. On the other hand, the current astrophysical observations also have exhibited that the distribution of matter is isotropic and the geometry of the present universe is in the form of spherical symmetry. However, it is also quite clear that at the early stage of evolution the universe could not have such a smoothed picture. Keeping this aspect in mind, in the present study we confine ourselves to construct the model of an inhomogeneous universe by considering the metric polynomials as function of the space and time both.

At theoretical point of view, the inhomogeneous cosmological models are too impartant mainly due to the following two reasons: (i) less validity of isotropic distribution of matter closure to the big bang impulse, and (ii) Perturbation present in the standard cosmological model. Firstly, Tolman [2] and thereafter other scientists, viz. Bondi [3], Taub [4,5], Tomimura [6], Szekeres [7] and Senovilla [8] have time to time constructed variety of plane symmetric inhomogeneous cosmological models through the exact solution of Einstein's general relativistic field equations. Later on, Ruis and Senovilla [8] have presented a significant work which is

singularity-free inhomogeneous cosmological model. Further Bali and Tyagi [9] and Pradhan et al. [10,11] have extended their studies on the plane symmetric inhomogeneous cosmological model under the Einstein-Maxwell space-time. Recently, Pradhan et al. [12], Yadav [13], Ali and Yadav [14] and Ali et al. [15] have also investigated various inhomogeneous cosmological models taking into consideration of different physical aspects.

In 1983, Zeldovich et al. [16] had been investigated the effect of magnetic field on galactic scale that gives clue for the importance of magnetic field for different astrophysical phenomenon. Harrison [17] has also discussed some applications of magnetic field in cosmology which motivate us to include magnetic field in the right side of Einstein's equation. In the recent past, the results of WMAP data are in favour of anisotropic modelling of universe. Some authors [18,19] have speculated that the occurance of a primordial magnetic field is bounded to some anisotropic models of universe spacially in case of *B-I*, *II*, *III*, VI_0 and VII_0. In this connection Zeldovich [20] and Barrow [21] have investigated that the magnetized anisotropic pressure dominates over the evolution caused by shear anisotropy. However, the existence of such field may possible at the end of an inflationary epoch as argue by several authors [22–24]. All the above studies indicate that the magnetized anisotropic models of universe play significant role in the evolving process of galaxies as well as stellar systems.

The Symmetry analysis method is a powerful tool for solving these equations [25–28]. These methods have been successfully applied in the area of theoretical physics, in particular quantum mechanics, fluid dynamics and particle physics [29,31]. We have elaborated this technique in the area of relativistic cosmology. Some applications of the Lie point symmetry analysis methods are discussed by Ali et al. [14,15]. For more details of the Lie groups, one may consult the following works [29,32,33] which deal with several applications including reduction of order of PDEs, development of similarity solution and generating new solutions from known ones. The classification of group-invariant solutions of differential equations by means of the so-called optimal system is one of the main applications of Lie group analysis of differential equations. The method was first conceived by Ovsiannikov [26]. In 1985, Ibragimov [31] has given some examples of optimal system in his book. Later on, Olver [27] has summarized some interesting discussion on similarity solution based on optimal systems.

In the present study, therefore, our goal is to search for an effective method for solving the system of nonlinear PDEs. This methodology we employ for accelerating universe in the plane symmetric space-time filled with non-exotic matter and electromagnetic fluid under general relativistic background. The outline of our study is as follows: in Sec. 2 we introduce the mathematical modeling of the accelerating universe in the plane symmetric space-time whereas Sec. 3 deals with the solution of the field equations. In Sec. 4 we provide some studies of physical and geometrical properties of our models and its validity. A few comments with a short discussion are presented in Sec. 5.

2. The Einstein-Maxwell spacetime geometry

The line element considered here is as follows

$$ds^2 = A^2\left(dx^2 - dt^2\right) + B^2dy^2 + C^2dz^2, \tag{1}$$

where the metric potentials A, B and C are functions of the spatial and temporal coordinates x and t both.

The usual form of energy-momentum tensor is given by

$$T_{\nu}^{\iota} = (\rho + p)v_{\nu}v^{\iota} + pg_{\nu}^{\iota} + E_{\nu}^{\iota}, \tag{2}$$

where E_{ν}^{ι} is the electromagnetic field and it is read as

$$E_{\nu}^{\iota} = \bar{\mu}\left[\zeta_{\ell}\zeta^{\ell}(v_{\nu}v^{\iota} + \frac{1}{2}g_{\nu}^{\iota}) - \zeta_{\nu}\zeta^{\iota}\right]. \tag{3}$$

In above equations the parameters ρ, p, v^{ι}, $\bar{\mu}$ and ζ_{ℓ} are the energy density, isotropic pressure, flow vector, magnetic permeability and magnetic flux vector respectively where

$$\zeta_{\ell} = \frac{1}{\bar{\mu}} \ {}^{*}F_{\iota\nu}v^{j}. \tag{4}$$

Again, the dual electro-magnetic field tensorSynge1960 is given by

$${}^{*}F_{\nu\iota} = \frac{\sqrt{-g}}{2}\epsilon_{\nu\iota k\ell}F^{k\ell}. \tag{5}$$

Here, we assume the current is flowing along z axis and F_{12} is the only non-vanishing component of electro-magnetic field tensor and the Maxwell equations are read as

$$\left[\frac{1}{\bar{\mu}}F^{\iota\nu}\right]_{;\iota} = 0, \tag{6}$$

where the semicolon (;) stands for their usual meaning, i.e. the matter creation through non-zero left hand side is possible while conserving the over all energy and momentum.

The Maxwell equation (6) leads to $\frac{\partial}{\partial x}\left[\frac{F_{12}(x,t)C(x,t)}{\bar{\mu}(x,t)B(x,t)}\right]$ $= 0$ which requires that

$$\frac{F_{12}(x,t)C(x,t)}{\bar{\mu}(x,t)B(x,t)} = f(t), \tag{7}$$

where $f(t)$ is an arbitrary function of t and we assume the component F_{12} of the electromagnetic field and the magnetic permeability $\bar{\mu}$ as a functions of x and t both.

The Einstein field equations are read as

$$R_{i}^{j} - \frac{1}{2}Rg_{i}^{j} = -8\pi T_{i}^{j}, \tag{8}$$

Solving Eq. (1) with Eq. (8), one obtain

$$E_1 = \frac{B_{xt}}{B} + \frac{C_{xt}}{C} - \frac{A_t}{A}\left(\frac{B_x}{B} + \frac{C_x}{C}\right) - \frac{A_x}{A}\left(\frac{B_t}{B} + \frac{C_t}{C}\right) = 0, \tag{9}$$

$$E_2 = \frac{B_tC_t - B_xC_x}{BC} + \frac{B_{tt}}{B} + \frac{C_{xx}}{C} + \frac{A_{xx} - A_{tt}}{A} + \frac{A_t}{A}\left(\frac{A_t}{A} - \frac{B_t}{B} - \frac{C_t}{C}\right) - \frac{A_x}{A}\left(\frac{A_x}{A} + \frac{B_x}{B} + \frac{C_x}{C}\right) = 0, \tag{10}$$

$$\chi A^2 p(x,t) = \frac{B_{xx}-2B_{tt}}{2B} - \frac{C_{tt}}{2C} + \frac{A_{xx}-A_{tt}}{2A} + \frac{B_xC_x - B_tC_t}{2BC} + \frac{A_t}{2A}\left(\frac{A_t}{A}+\frac{B_t}{B}+\frac{C_t}{C}\right) - \frac{A_x}{2A}\left(\frac{A_x}{A}-\frac{B_x}{B}-\frac{C_x}{C}\right), \quad (11)$$

$$\chi A^2 \rho(x,t) = \frac{C_{tt}-2C_{xx}}{2C} - \frac{B_{xx}}{2B} + \frac{A_{xx}-A_{tt}}{2A} + \frac{3\left(B_tC_t - B_x\,C_x\right)}{2BC} + \frac{A_t}{2A}\left(\frac{A_t}{A}+\frac{B_t}{B}+\frac{C_t}{C}\right) + \frac{A_x}{2\,A}\left(\frac{A_x}{A}+\frac{B_x}{B}+\frac{C_x}{C}\right), \quad (12)$$

$$\frac{\chi F_{12}^2(x)}{B^2\bar{\mu}(x,t)} = \frac{B_xC_x - B_tC_t}{BC} - \frac{C_{tt}}{C} - \frac{B_{xx}}{B} + \frac{A_{tt}-A_{xx}}{A} + \frac{A_t}{A}\left(\frac{C_t}{C}+\frac{B_t}{B}-\frac{A_t}{A}\right) + \frac{A_x}{A}\left(\frac{A_x}{A}+\frac{B_x}{B}+\frac{C_x}{C}\right) \quad (13)$$

The scalar expansion Θ and shear scalar σ^2 can be provided as:

$$\Theta = \frac{1}{A}\left(\frac{A_t}{A}+\frac{B_t}{B}+\frac{C_t}{C}\right), \quad (14)$$

$$\sigma^2 = \frac{\Theta^2}{3} - \frac{1}{A^2}\left(\frac{A_tB_t}{AB}+\frac{A_tC_t}{AC}+\frac{B_tC_t}{BC}\right). \quad (15)$$

In Eqs. (9)-(13), there are five highly non-linear differential equations with six unknown variables, viz. A, B, C, p, ρ and $F_{12}^2/\bar{\mu}$. In general, it is impossible to solve these equations without assuming physically reasonable conditions amongst the parameters. In the present situation for the model (1), let us assume that $\Theta \propto \sigma_1^1$ which leads to the relation between the metric potentials as follows:

$$\frac{2A_t}{A} - \frac{B_t}{B} - \frac{C_t}{C} = 3\delta\left(\frac{A_t}{A}+\frac{B_t}{B}+\frac{C_t}{C}\right), \quad (16)$$

where δ is a proportional constant.

Equation (16) can be written in the following convenient form

$$\frac{A_t}{A} = n\left(\frac{B_t}{B}+\frac{C_t}{C}\right), \quad (17)$$

where $n = \frac{1+3\delta}{2-3\delta}$.

Integrating it with respect to t, we obtain

$$A(x,t) = f(x)B^n(x,t)C^n(x,t), \quad (18)$$

where $f(x)$ is an integration constant and has an arbitrary functional relationship with x.

Equations (18), (9) and (10) lead the following equations

$$E_1 = \frac{B_{xt}}{B} + \frac{C_{xt}}{C} - 2n\left(\frac{B_xB_t}{B^2} + \frac{B_xC_t+B_tC_x}{BC} + \frac{C_xC_t}{C^2}\right) - \frac{f'}{f}\left(\frac{B_t}{B}+\frac{C_t}{C}\right) = 0, \quad (19)$$

$$E_2 = n\left(\frac{B_{xx}}{B} - \frac{C_{tt}}{C}\right) + (1-n)\frac{B_{tt}}{B} + (1+n)\frac{C_{xx}}{C} + 2n\left(\frac{B_x^2}{B^2} - \frac{C_x^2}{C^2}\right) + (1-2n)\frac{B_t C_t}{BC} - (1+2n)\frac{B_x C_x}{BC} - \frac{f'}{f}\left(\frac{B_x}{B} + \frac{C_x}{C}\right) + \frac{ff'' - f'^2}{f^2} = 0. \quad (20)$$

Here and in what follows, a prime indicates derivative with respect to the coordinate x.

3. The solutions of the Einstein-Maxwell field equations

If we solve the system of second order nonlinear partial differential equations (NLPDEs) involved in Eqs. (19)-(20), we shall get the exact solution of the problem under consideration. Several authors [34–36] have adopted a simple approach to obtain exact solution by taking into account $B(x,t) = B_1(x)B_2(t)$ and $C(x,t) = C_1(x)C_2(t)$. However, in the present paper we have investigated for a new solution by using the symmetry analysis method [26,27,29,30] and optimal system [26,27]. It is to note that a complete description of the methods to solve NLPDEs in the framework of general relativity are available in the following works [37,15].

Thus for metric (1), the components of symmetries are given by

$$\xi_1 = c_1 x + c_2,\ \xi_2 = c_1 t + c_3,\ \eta_1 = c_4 B,\ \eta_2 = c_5 C, \quad (21)$$

where the function $f(x)$ must be taken the following forms

$$\begin{cases} f(x) = c_6 \exp\left[c_7 x\right], & \text{if} \quad c_1 = 0, \\ f(x) = c_8\left(c_1\, x + c_2\right)^{c_9}, & \text{if} \quad c_1 \neq 0, \end{cases} \quad (22)$$

with c_i an arbitrary constant where $i = 1, 2, ..., 9$.

The equation (22) leads the following optimal systems

$$\begin{cases} X^{(1)} = X_1 + c_4 X_4 + c_5 X_5, \\ X^{(2)} = c_2 X_2 + X_3 + c_4 X_4 + c_5 X_5, \\ X^{(3)} = X_2 + c_4 X_4 + c_5 X_5, \\ X^{(4)} = X_4 + c_5 X_5, \\ X^{(5)} = X_5 \end{cases} \quad (23)$$

In the present work our procedure of solving the NLPDEs is similar to the works [37,15] but here the source of the energy-momentum tensor and explicit expressions of all the cosmological parameters are entirely different. Basically in this study we have presented a model of accelerating universe filled with perfect fluid and electromagnetic field in the framework of inhomogeneous plane symmetric space-time. To our knowledge, this is the first study that deals with the inhomogeneous modelling of accelerating universe by taking into account the perfect fluid and electromagnetic field as the source of matter-energy density.

The characteristic equations for symmetries (21) are read as

$$\frac{dx}{c_1 x + c_2} = \frac{dt}{c_1 t + c_3} = \frac{dB}{c_4 B} = \frac{dC}{c_5 C}. \quad (24)$$

From Eq. (23), it is to be noted that $c_1 = c_3 = 0$ for symmetries $X^{(3)}$, $X^{(4)}$ or $X^{(5)}$. Also Eq. (24) leads to the similarity variable as $\xi = t$, where B and C have functional relations with t. Therefore, invariant solutions are possible only for the following two cases:

Case I - Symmetries $X^{(2)}$: From Eq. (24), with $c_1 = 0$ and $c_3 = 1$, we have

$$\begin{aligned} &\xi = x + bt,\ B(x,t) = \varphi(\xi)\exp[cx], \\ &C(x,t) = \phi(\xi)\exp[dx], \end{aligned} \tag{25}$$

where $b = -c_2$, $c = \frac{c_4}{c_2}$ and $d = \frac{c_5}{c_2}$ are arbitrary constants.

Case II - Symmetries $X^{(1)}$: From Eq. (24), with $c_1 = 1$ and $c_2 = c_3 = 0$, we have

$$\xi = \tfrac{t}{x},\ B(x,t) = x^c\varphi(\xi),\ C(x,t) = x^d\phi(\xi), \tag{26}$$

where $c = c_4$ and $d = c_5$ are arbitrary constants.

However, one can perform mathematical and physical analysis by considerding several subcases under the above two cases and conclude that *Case I* and some of its subcases lead us to the physically interesting and viable solutions. Therefore, to save time as well as space, we shall consider only *Case I* and following subcases in our calculations.

Hence, substitution of the transformations (25) in Eqs. (19)-(20) provide

$$\Big[c_7 - c + 2n(d-c)\Big]\frac{\varphi'}{\varphi} + \Big[c_7 - d + 2n(c-d)\Big]\frac{\phi'}{\phi} + 2n\Big(\frac{\varphi'}{\varphi} + \frac{\phi'}{\phi}\Big)^2 - \frac{\varphi''}{\varphi} - \frac{\phi''}{\phi} = 0, \tag{27}$$

$$\begin{aligned} &\Big[(n-1)b^2 - n\Big]\frac{\varphi''}{\varphi} - \Big[n + 1 - nb^2\Big]\frac{\phi''}{\phi} + 2n\Big(\frac{\varphi'^2}{\varphi^2} + \frac{\phi'^2}{\phi^2}\Big) + \\ &\Big[2n + 1 + (2n-1)b^2\Big]\frac{\varphi'\phi'}{\varphi\phi} + \Big[c_7 + d + 2n(c+d)\Big]\frac{\varphi'}{\varphi} + \\ &\Big[c_7 + d + 2n(c+d) - 2a_4\Big]\frac{\phi'}{\phi} + d(c-d) + c_7(c+d) + n(c+d)^2 = 0. \end{aligned} \tag{28}$$

Eqs. (27) and (28) being difficult to solve one may consider a special case with $b = -1$. Therefore, subtracting in Eq. (27) and (28), we get

$$\tfrac{\phi'}{\phi} + \tfrac{(c+d)\varphi'}{(c-d)\varphi} = \alpha_0, \tag{29}$$

where $\alpha_0 = \frac{d(c_7-d)+c(c_7+d)+n(c+d)^2}{d-c}$.

After integration the above equation with respect to ξ, we obtain

$$\phi(\xi) = r_1\varphi^{\alpha_1}(\xi)\exp[\alpha_0\xi], \tag{30}$$

where $\alpha_1 = \frac{d+c}{d-c}$ while r_1 is an arbitrary integration constant.

The equation (27), after using the transformation

$$\varphi(\xi) = r_2\exp\Big[\alpha_2\int\Omega(\xi)d\xi\Big] \tag{31}$$

and (30), becomes

$$\Omega' = \eta_1\Omega^2 + \eta_2\Omega + \eta_3, \tag{32}$$

where

$$\begin{cases} \eta_1 = \dfrac{\alpha_2\left[(c^2+3d^2)(c^2+2cd-d^2)+4d^2[(c-d)\alpha_0+(c+d)c_7]\right]}{d(c-d)(c+d)^2}, \\ \eta_2 = \dfrac{c^4-8c^2d^2-4cd^3+3d^4-2\left[c^3+5c^2d+7cd^2-5d^3\right]\alpha_0+8d\alpha_0\left[(d-c)\alpha_0-(c+d)c_7\right]}{2d(c+d)^2} - c_7, \\ \eta_3 = \dfrac{\alpha_0(c-d)\left[2c(d+\alpha_0)(d+c_7+\alpha_0)-d(d-c_7+\alpha_0)(d+2\alpha_0)+c^2(3d+c_7+3\alpha_0)\right]}{2d\alpha_2(c+d)^2}, \end{cases} \tag{33}$$

and r_2 is constant while $\Omega(\xi)$ is a new function of ξ.

To get solution of the above ordinary differential equation we consider the following special cases: $\eta_1 \neq 0$, $\eta_2 = 0$ and $\eta_3 \neq 0$ so that the general solution to Eq. (32) becomes

$$\Omega(\theta) = \sqrt{\tfrac{\alpha_5}{\alpha_3}}\tan\left[\sqrt{\alpha_5\alpha_3}\xi\right]. \tag{34}$$

The above solution is very complicated because the values of α_3 and α_5 are very complicated. Therefore, we shall study the simple case as follows: $\alpha_0 = \frac{d^2}{2c} - \frac{3d}{2} - c$.

Now, using (34), (31), (30) and (25), and after some calculation, we can obtain the solutions of the metric functions in this case as follows:

$$\textbf{Case } (\mathbf{b-1}) : m > 3 + \frac{2}{m}$$

$$\begin{cases} A(x,t) = q_1 \exp\left[\dfrac{K\left[(2m^3-5m^2+m-2)x-(m^2-3m-2)t\right]}{\sqrt{2}(m-1)^2K_0}\right] \\ \qquad\qquad \times \cos^{\gamma_0}[\theta], \\ B(x,t) = q_2 \exp\left[\dfrac{2\sqrt{2}\gamma_0 Kx}{K_0}\right]\cos^{(m-1)\gamma_0}[\theta], \\ C(x,t) = q_3 \exp\left[\dfrac{\sqrt{2}\gamma_0 K\left[(m^2-m-2)x-(m^2-3m-2)t\right]}{K_0}\right] \\ \qquad\qquad \times \cos^{(m+1)\gamma_0}[\theta], \end{cases} \tag{35}$$

where $\gamma_0 = \frac{m}{(m-1)^2}$, $K_0^2 = m - 3 - \frac{2}{m}$, $f(x) = c_6\exp\left[\frac{\sqrt{2}K(m^3-3m^2+m-1)x}{K_0(m-1)^2}\right]$ and $\theta = K(x-t)$, the symbols K, m, q_1, q_2 and q_3 all are being arbitrary constants, however, here m will never be 0 or 1.

$$\textbf{Case } (\mathbf{b-2}) : m < 3 + \frac{2}{m}$$

$$\begin{cases} A(x,t) = q_1 \exp\left[\frac{K\left[(2m^3-5m^2+m-2)x-(m^2-3m-2)t\right]}{\sqrt{2}K_0(m-1)^2}\right] \\ \qquad \times \cosh^{\gamma_0}[\theta], \\ B(x,t) = q_2 \exp\left[\frac{2\sqrt{2}K\gamma_0 x}{K_0}\right] \cosh^{(m-1)\gamma_0}[\theta], \\ C(x,t) = q_3 \exp\left[\frac{\sqrt{2}K\gamma_0\left[(m^2-m-2)x-(m^2-3m-2)t\right]}{K_0}\right] \\ \qquad \times \cosh^{(m+1)\gamma_0}[\theta], \end{cases} \tag{36}$$

where $\gamma_0 = \frac{m}{(m-1)^2}$, $K_0^2 = \frac{2}{m} + 3 - m$, $f(x) = c_6 \exp\left[\frac{\sqrt{2}K(m^3-3m^2+m-1)x}{K_0(m-1)^2}\right]$, $\theta = K(x-t)$, the symbols K, m, q_1, q_2 and q_3 all are being arbitrary constants as above, however, here also m must never be 0 or 1.

4. Validity of the cosmological models: a special case study

As mentioned in the previous Sec. 3, we are now performing a study regarding different properties of the model in Eq. (50) under *subcase (b-1)*. One can observe that if we take $m = 0$ or 1, the values of the constants diverse to infinity. For this reason we have purposely skipped the **Case (b-2)** as this prescription represents a non-realistic model.

For this model, from the equation set (35), we get the following physical parameters

$$\rho(x,t) = \frac{2\sqrt{2}\gamma_0^2K^2}{\chi q_1^2K_0^2} \exp\left[\frac{\sqrt{2}K\left[(m^2-3m-2)t-(2m^3-5m^2+m-2)x\right]}{K_0(m-1)^2}\right] \times\left(\sqrt{2}(3+4m-m^3)+K_0(1+2m+3m^2)\tan[\theta]\right)\cos^{-2\gamma_0}[\theta], \tag{37}$$

$$p(x,t) = \frac{2\sqrt{2}\gamma_0^2K^2}{\chi q_1^2K_0^2} \exp\left[\frac{\sqrt{2}K\left[(m^2-3m-2)t-(2m^3-5m^2+m-2)x\right]}{K_0(m-1)^2}\right] \times\left(\sqrt{2}(m^3-2m^2-2m+1)+K_0(1-2m-m^2)\tan[\theta]\right) \times\cos^{-2\gamma_0}[\theta], \tag{38}$$

$$\frac{F_{12}^2(x,t)}{\bar{\mu}(x,t)} = \frac{4\sqrt{2}m^2q_2^2K^2\exp\left[4\sqrt{2}\gamma_0Kx/K_0\right]}{\chi(m-1)^4K_0^2\cos^{(2-2m)\gamma_0}[\theta]} \times \left(\sqrt{2}(m^3-2m^2-2m-1)-K_0(m^2+1)\tan[\theta]\right), \tag{39}$$

where ρ, p and $\bar{\mu}$ are the energy density, pressure and magnetic permeability respectively with $\gamma_0 = \frac{m}{(m-1)^2}$, $\theta = K(x-t)$.

Now, by considering the condition (7), we have

$$\bar{\mu}(x,t) = \frac{4K^2\gamma_0^2q_3^2}{K_0^2\chi f(t)} \exp\left[\frac{2\sqrt{2}K\gamma_0\left[(m^2-m-2)x-(m^2-3m-2)t\right]}{K_0}\right] \times\left(2m^3-4m^2-4m-2-\sqrt{2}K_0(m^2-1)\tan[\theta]\right)\cos^{2\gamma_0(m+1)}[\theta], \tag{40}$$

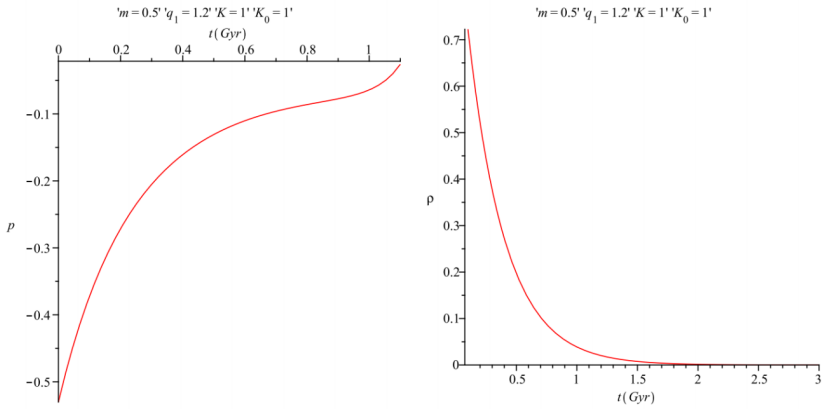

Fig. 1 Variation of the fluid pressure and matter-energy density with respect to the age of the universe t for the specified values of the constants of the model.

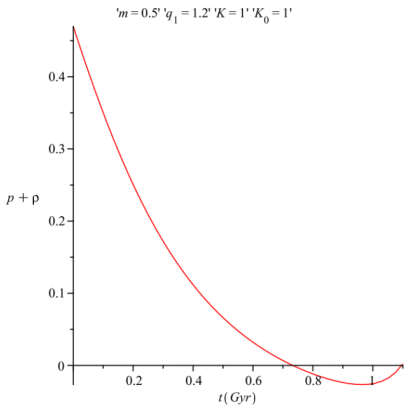

Fig. 2 Variation of the null energy condition $p+\rho$ with respect to the age of the universe t for the specified values of the constants of the model.

$$F_{12}(x,t) = -\frac{4K^2\gamma_0^2 q_3 q_2}{K_0^2 \chi\sqrt{f(t)}} \exp\left[\frac{\sqrt{2}K\gamma_0\left[(m^2-m)x-(m^2-3m-2)t\right]}{K_0}\right] \times\left(2m^3-4m^2-4m-2-\sqrt{2}K_0(m^2-1)\tan[\theta]\right)\cos^{2m\gamma_0}[\theta], \tag{41}$$

In Fig. 1 we have drawn the behaviour for p and ρ which show the expected evolutionary features of the universe.

By using the expressions of density (Eq. 37) and pressure (Eq. 38) we also draw plot for $p+\rho$ in Fig. 2. This figure indicates that the null energy condition

(i.e. $\rho + p \geq 0$) is obeyed by the system in the early time, however violates at the later stage which supports a deceleration to acceleration feature of the universe.

Now, the expressions for the volume element (V), expansion scalar (Θ), shear tensor (σ_i^j) and shear scalar (σ^2) are given by

$$V = q_1^2 q_2 q_3 \ \cos^{(2m+2)\gamma_0}[\theta] \ \exp\left[\frac{\sqrt{2}K\Big[(2+5m+2m^2-m^3)t-(2-m+6m^2-3m^3)x\Big]}{(m-1)^2K_0}\right] \tag{42}$$

$$\Theta = \frac{(2m+1)\gamma_0 K\left(\sqrt{2}\tan[\theta]-K_0\right)}{\sqrt{2}q_1\cos^{\gamma_0}[\theta]} \exp\left[\frac{K\Big[(m^2-3m-2)t-(2m^3-5m^2+m-2)x\Big]}{\sqrt{2}K_0(m-1)^2}\right]. \tag{43}$$

$$\begin{cases} \sigma_1^1 = \left(\frac{1}{1+2m}-\frac{1}{3}\right)\Theta, \\ \sigma_2^2 = \frac{1}{3+6m}\left(\frac{(2+7m+5m^2-2m^3)-\sqrt{2}(m^2-4m)K_0\tan[\theta]}{(m^2-3m-2)-\sqrt{2}mK_0\tan[\theta]}\right)\Theta, \\ \sigma_3^3 = -\Big(\sigma_1^1+\sigma_2^2\Big). \end{cases} \tag{44}$$

$$\sigma^2 = \frac{m^2-3m-2}{6(1+2m)^2}\left(\frac{\delta_0+\delta_1\cos[2\theta]-2\sqrt{2}m(m^2+m+1)K_0\sin[2\theta]}{\Big[(m^2-3m-2)\cos[\theta]-\sqrt{2}mK_0\sin[\theta]\Big]^2}\right)\Theta^2, \tag{45}$$

where $\delta_0 = 4m^4 - 12m^3 - 5m^2 + 9m - 2$ and $\delta_1 = 4m^4 - 16m^3 + 3m^2 - 7m - 2$.

On the other hand, non-vanishing acceleration and rotation components are computed as

$$\begin{cases} \dot{u}_1 = \frac{K}{\sqrt{2}(m-1)^2K_0}\Big(\delta_2-\sqrt{2}mK_0\tan[\theta]\Big), \\ \omega_{41} = -\omega_{14} = \frac{q_1K\left(\delta_2-\sqrt{2}mK_0\tan[\theta]\right)}{\sqrt{2}(m-1)^2K_0} \times \exp\left[\frac{K\Big[\delta_2 x-(m^2-3m-2)t\Big]}{\sqrt{2}(m-1)^2K_0}\right]\cos^{\gamma_0}[\theta], \end{cases} \tag{46}$$

where $\delta_2 = 2m^3 - 5m^2 + m - 2$.

Following the work of Feinstein and lbanez [38] and Raychaudhuri [39] the deceleration parameter is given by

$$\begin{aligned} \mathbf{q} = &\frac{\gamma_0(1+2m)^3K^4\left(\delta_3+\sqrt{2}mK_0\tan[\theta]\right)^2}{4q_1^4(1-m)^5K_0^2}\exp\left[\frac{2\sqrt{2}K\Big[\delta_3 t-\delta_2 x\Big]}{(m-1)^2K_0}\right]\cos^{-2-4\gamma_0}[\theta] \\ &\times\Big[m^2-7m+4+(m^2-5m-2)\cos[2\theta]-2\sqrt{2}mK_0\sin[2\theta]\Big], \end{aligned} \tag{47}$$

where $\delta_3 = m^2 - 3m - 2$.

The deceleration parameter q is ploted in Fig. 3 which interestingly indicates a change over from the positive q to the negative q with evolution of the universe, i.e. in physical sense from deceleration to accelerating universe. Therefore, the figure actually reveals two particlar features: (i) there is a flip-flop which indicates a slow rolling down of the phase of universe from dceleration to acceleration, and (ii) the

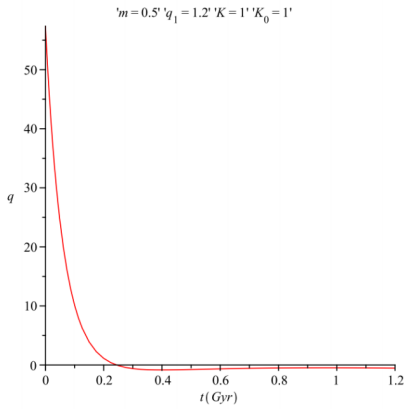

Fig. 3 Variation of the deceleration parameter q with respect to the age of the universe t for the specified values of the constants of the model.

phase of acceleration from deceleration has been started from around $t = 0.29$ Gyr. In the present epoch of an accelerating universe, q lies near -0.50 ± 0.05 (see the following works [40–43]. From our model, we can recover $q = -0.5$ for $t = 0.244$ Gyr when deceleration to acceleration occurs whereas we got $q = -0.5$ at $t = 0.29$ Gyr after fine tuning it. However, this data for time seems very low as literature suggests a probable much higher value for t as ~ 6 Gyr [44–49].

5. Conclusion

In the present study, the Lie symmetry analysis has been executed under the Einstein's general relativistic background and hence construction of models for the accelerating universe with perfect fluid and electromagnetic field has been done in plane symmetric spacetime.

Some interesting and viable physical features of the studies are as follows:

(1) In the present investigation the free gravitational field is assumed to be of the Petrov type-II non-degenerate which provides physically interesting results.

(2) The study deals with the electromagnetic energy of the inhomogeneous universe. The electromagnetic field tensor (F_{12}) is found to be positive and increasing function of time.

(3) Among the models presented in Sec. 3 only the case studied in Sec. 4 is found to be interesting with temporial behaviour as far as plots and data are concerned. Other models are with unrealistic physical features having either positive density and volume decreasing or volume increasing but density is negative.

(4) The deceleration parameter q as ploted in Fig. 3 interestingly indicates a change over from positive q to negative q with evolution of the universe i.e. from deceleration to accelerating universe. From our model, we obtain presently accepted numerical value of q as -0.5 for $t = 0.24$ Gyr. However, this value of age seems very low with respect to $t \sim 6$ Gyr as available in literature [44–49].

As a final comment we would like to put our overall observations of the present study as follows: qualitatively (see Figs. 1-3) the model under plane-symmetric

Einstein-Maxwell spacetime is very promising though quantitative result (q from Fig. 3) seems does not fit for the observed data. This readily indicates that either the analysis under plane symmetric spacetime is not fully compatible with the observable universe or probably we have missed some of the threads in our whole consideration which are responsible to make the analysis partially compatible.

Acknowledgments

SR is grateful to the IUCAA, Pune as well as IMSc, Chennai, India for providing Visiting Associateship under which a part of this work was carried out. FR is also grateful to the IUCAA, Pune, India for providing Visiting Associateship scheme and to SERB, DST for financial support. AM is thankful to DST for financial support under INSPIRE scheme.

References

1. A.G. Walker, *Proc. London Math. Soc.*, **42** (1937) 90.
2. R.C. Tolman, *Proc. Nat. Acad. Sci.*, **20** (1934) 169.
3. H. Bondi, *Mon. Not. R. Astro. Soc.*, **107** (1947) 410.
4. A.H. Taub, *Ann. Math.*, **53** (1951) 472.
5. A.H. Taub, *Phys. Rev.*, **103** (1956) 454.
6. N. Tomimura, *Nuo. Cim. B*, **44** (1978) 372.
7. P. Szekeres, *Commun. Math. Phys.*, **41** (1975) 55.
8. J.M.M. Senovilla, *Phys. Rev. Lett.*, **64** (1990) 2219.
9. R. Bali and A. Tyagi, *Astrophys. Space Sc.*, **173** (1990) 233.
10. A. Pradhan, A.K. Yadav and J.P. Singh, *Fizika B*, **16** (2007) 175.
11. A. Pradhan, P.K. Singh and A.K. Yadav, *Commun. Theor. Phys.*, **54** (2010) 191.
12. A. Pradhan, M.K. Mishra and A.K. Yadav, *Rom. J. Phys.*, **54** (2009) 747.
13. A.K. Yadav, *Int. J. Theor. Phys.*, **49** (2010) 1140.
14. A.T. Ali and A.K. Yadav, *Int. J. Theor. Phys.*, **53** (2014) 2505.
15. A.T. Ali, A.K. Yadav, F. Rahaman and A. Mallick, *Phys. Scr.*, **89** (2014) 115206.
16. Ya.B. Zeldovich, A.A. Ruzmainkin and D.D. Sokoloff, *Magnetic field in Astrophysics*, Gordon and Breach, New Yark (1983).
17. E.R. Harrison, *Phys. Rev. Lett.*, **30** (1973) 188.
18. E. Asseo and H. Sol, *Phys. Rep.*, **148** (1987) 307.
19. L.P. Hughston, K.C. Jacobs, *Astrophys. J.*, **160** (1970) 147.
20. Ya.B. Zeldovich, *Sov. Astron.*, **13** (1970) 608.
21. J.D. Barrow, *Phys. Rev. D*, **55** (1997) 7451.
22. M.S. Turner and L.M. Widrow, *Phys. Rev. D*, **30** (1988) 2743.
23. J. Quashnock, A. Loeb and D.N. Spergel, *Astrophys. J.*, **344** (1989) L49.
24. A.D. Dolgov, *Phys. Rev. D*, **48** (1993) 2499.
25. G.W. Bluman and S. Kumei, *Symmetries and differential equations in applied sciences*, Springer, New York (1989).
26. L.V. Ovsyannikov, *Group Analysis of Differential Equations*, Academic Press, New York (1982).
27. P.J. Olver, *Application of Lie Groups to differential equations*, New York: Springer (1993).
28. Z. Zhang, B. Gao and Y. Chen, *Commun. Nonlinear. Sci. Numer. Simul.*, **16** (2011) 2709.
29. G. Baumann, *Symmetry Analysis of Differential Equations with Mathematica*, Telos, Springer Verlag, New York (2000).
30. G.W. Bluman and S.C. Anco, *Symmetry and Integration Method for Differential Equations*, Springer Verlag, New York (2002).
31. N.H. Ibragimov, *Transformation groups applied to mathematical physics*, Reidel, Dordrecht (1985)
32. P.J. Olver, Equivalence, *Invariants and Symmetry*, Cambridge University Press, Cambridge (1995).

33. H. Stephani, *Differential Equations: Their Solutions Using Symmetries*, Cambridge University Press (1989).
34. A. Pradhan, A.K. Yadav, R.P. Singh and V.K. Singh, *Astrophys. Space Sci.*, **312** (2007) 145.
35. A.K. Yadav, V.K. Yadav and L. Yadav, *Int. J. Theor. Phys.*, **48** (2009) 568.
36. A.T. Ali and F. Rahaman, *Int. J. Theor. Phys.*, **52** (2013) 4055.
37. A.K. Yadav and A.T. Ali, *Eur. Phys. J. Plus*, **129** (2014) 179.
38. A. Feinstein and J. lbanez, *Class. Quantum Gravit.*, **10** (1993) L227.
39. A.K. Raychaudhuri, *Theoritical Cosmology*, Oxford (1979).
40. R. Tripp, *Astron. Astrophys.*, **325** (1997) 871.
41. J.M. Overduin and F.I. Cooperstock, *Phys. Rev. D*, **58**, (1998) 043506.
42. G. Efstathiou et al., Arxiv: astro-ph/9812226.
43. V. Sahni, *Pramana - J. Phys.*, **53** (1999) 937.
44. A.G. Riess et al., *Astron. J.*, **116** (1998) 1009.
45. S. Perlmutter et al., *Nature*, **391** (1998) 51.
46. D.N. Spergel et al., *Astrophys J. Suppl.*, **148** (2003) 175.
47. R.P. Kirshner, *Science*, **300**, (2003) 1914.
48. M. Tegmark et al., *Phys. Rev. D*, **69** (2004) 103501.
49. S. Ray, U. Mukhopadhyay and X.-H. Meng, *Gravit. Cosmol.*, **13** (2007) 142.

Scientific Voyage
Vol. 1, No. 1
page 39-44 (2020)

SCIENTIFIC VOYAGE
ISSN: 2395-5546

ISSN: 2395-5546

A Discussion on Variants of Heuristic Algorithms for Flow Shop Scheduling Problem

Partha Haldar[1,*], Alok Mukherjee[2] and Kingshuk Chatterjee[3]

[1]*Mechanical Engineering, Government College of Engineering and Ceramic Technology, Kolkata 700 010, West Bengal, India*

[2] *Electrical Engineering, Government College of Engineering and Ceramic Technology, Kolkata 700 010, West Bengal, India*

[3]*Computer Science and Engineering, Government College of Engineering and Ceramic Technology, Kolkata 700 010, West Bengal, India*

Flowshop scheduling is a fundamental task in any industry related to production. An optimized schedule ensures efficient generation of products and minimization of waiting time. In this paper, we present a review of the different variants of the flowshop problem and also discuss some of the interesting heuristic algorithms employed to solve the practical problems.

Keywords: Flowshop problem, permutation, scheduling, continuous, block, heuristic algorithms.

1. Introduction

The flowshop scheduling problem involves n number of jobs and *m* no of machines. The jobs must pass through the m machines in a particular fixed order. The objective of the flowshop scheduling problem is to find a schedule which minimizes the total time of execution of the jobs (makespan). There are number of variations of the flowshop scheduling problem viz., permutation flowshop scheduling, continuous flowshop scheduling and block flowshop scheduling. The flowshop scheduling problem has been shown to be NP-hard which essentially means that an optimal solution to this problem is very difficult and is most likely to take exponential time. As a result, the algorithms that have been developed to solve the flowshop problem, try to obtain a near optimal solution using various methods such as heuristics, approximate algorithms and soft computing tools such as GAs. Many detailed survey of the flowshop scheduling problem are already present in the literature, and they are not up to date and do not discuss the latest algorithms associated with this field. In this paper, we incorporate the very recent heuristic based algorithms and works along with the already existing algorithms in this field. The main objectives of this paper are as follows:

1. To discuss the different variants of the flowshop scheduling problem
2. To discuss the different types of heuristic based algorithms employed to solve the flowshop scheduling problem.

2. Preliminaries

This section contains the basic definitions of the different variants of flowshop scheduling. These are briefed as follows:

2.1 Permutation flowshop scheduling:

In the case of permutation flowshop scheduling problem, there are n jobs that have to be performed on m unrelated
machines and every job consists of m non-preemptible operations. Every operation of a job uses a different machine

*corresponding author: partha.haldar@gcect.ac.in

during a given time and may wait before being processed. For the permutation flow shop problem, the operations of every job must be processed on machines 1 , . . . , m in this order. Moreover, the processing order of the jobs on the
machines is the same for every machine. The problem consists in finding a permutation of the n jobs that minimizes the makespan.

2.2 Continuous flowshop scheduling:

The continuous flow-shop scheduling problem has the additional restriction that the processing of each job has to be continuous, i.e., once the processing of a job begins, there must not be any waiting times between the processing of any consecutive tasks of this job. Such a no-wait constraint is usually due to technological restrictions of the production process.

2.3 Blocked flowshop scheduling:

Blocked flowshop scheduling is a flowshop where a job having completed processing on a machine cannot leave this machine until its next machine is available for processing. That is, the job will block the current machine if its next machine is not available. The type of flowshop scheduling problem without intermediate buffers are known as the blocking flowshop scheduling problem. In the literature, the most common criterion for the blocking flowshop problem is the minimization of the makespan or the maximum completion time of the schedule.

3. Review of Heuristics Algorithms to solve flowshop scheduling problems:

In this section, we focus on the different heuristics techniques proposed by different authors to obtain near optimal solution to the flowshop scheduling problem. We discuss in brief, the different methods and modifications of some renowned heuristics algorithms in the next section. Heuristic Method is the most popular algorithmic technique to solve the flowshop scheduling problem. Various different types of heuristics have been used but the most popular heuristic that have been used is to arrange the jobs in ascending or descending order of their execution time.

Allahverdi et. al. [1] developed a new heuristics to minimize total completion time in m-machine flowshop problem. In this paper, the authors compare few heuristics that are independently developed and they propose several new heuristic methods modifying the existing heuristics models such as CDS heuristic [2], NEH heuristic [3], HO heuristic [4],Wang et al. heuristic [5], RZ heuristic [6] and WY heuristic [7]. Their analysis shows that a small proposed modification (pairwise exchange) improves the error performance of the best existing algorithms almost 50% with negligible CPU time.

Fink and Stefan [8] describes a method of solving the continuous flow-shop scheduling problem by metaheuristics. They examine the trade-off between running time and solution quality. They also investigate the knowledge and efforts needed to implement and calibrate their algorithms. They show that high quality results could be achieved in an efficient way by applying metaheuristics software components with neither the need to understand their inner working nor the necessity to manually tune parameters.

Framinan and Leisten [9] propose a heuristic for mean/total flowtime minimization in permutation flow shops. The heuristic exploits the idea of 'optimizing' partial schedules, already present in the NEH-heuristic [3] with respect to makespan minimization. Their experiment shows that their proposed heuristic model outperforms some existing best performing heuristics with respect to the quality of the solutions. The proposed model could further be embedded in an improvement scheme to build a composite heuristic for the flow time minimization problem.

Framinan and Leisten [9] represents an exhaustive review and comparative evaluation of heuristics and metaheuristics for the well-known permutation flowshop problem with the makespan criterion. They propose a comparison of 25 existing heuristics methods, ranging from the classical Johnson's algorithm or dispatching rules to the most recent metaheuristics, including taboo search, simulated annealing, genetic algorithms, iterated local search and hybrid techniques. The authors use the experimental design approach to validate the effectiveness and efficiency of the different methods.

Taillard [10] explains the problem of sequencing jobs in a permutation flow shop problem with an aim of minimizing the sum of flowtime, which is very much relevant to the latest dynamic production environment, and therefore it has attracted the attention of researchers during the last few years. Hence, a variety of heuristics have recently been developed, each claiming to be the best for the problem. The authors classify and conduct an extensive comparison among the existing heuristics, followed by analyzing the results of the experiments. They also suggest two new composite heuristics for the problem, which are proved very efficient for the problem.

Taillard [10] elaborates an efficient stochastic hybrid heuristic model for flowshop scheduling in order to minimize the makespan objective. Three probabilistic hybrid heuristics are proposed by the authors for solving the same and outperform best-known existing heuristics, combining elements from both constructive heuristic search and a stochastic improvement technique. Stochastic methods used by the authors include simulated annealing (SA). Tests are carried out to validate the improvements.

Liu and Reeves [11] explains another flowshop scheduling problem with the objective of minimizing the total flowtime using constructive heuristic and two composite heuristics methods. Computational analysis is carried out with the benchmark problems of Taillard [10]. The two proposed composite heuristic models prove better than the composite heuristics of Liu and Reeves [11]. Statistical tests of significance are used to validate the improvement in solution quality.

Chakravarthy et. al. [12] suggests a heuristic for scheduling in a flowshop with the objective of both minimizing the makespan and maximum tardiness of a job. The heuristic proposed by the authors makes use of the simulated annealing technique and compares the improvement of the proposal against the existing heuristic for scheduling to serve the objectives. The results of the computational evaluation reveal that the proposed heuristic performs better than the existing methods.

Laha et. al. [13] suggests a constructive heuristic for the permutation flowshop scheduling problem with an aim to minimize total completion time. Population-based technique has been adopted by the authors and also the insertion rule similar to that presented in the NEH [3] heuristic for the makespan criterion. The authors compare the computational results against the heuristics suggested by Woo and Yim [7] for small and large problem sizes and the heuristic of Framinan and Leisten [9] for small and medium problem sizes and suggests that the proposed heuristics performs better. The time complexity of the proposed method is also found to be less than those required by the existing topologies.

Pan et. al. [14] considers minimizing makespan for a blocking flowshop scheduling problem. A constructive heuristic is initially presented by the authors to generate a good solution by combining the existing profile fitting approach and NEH heuristic in an effective way. Further, the authors propose a Memetic Algorithm (MA) including effective techniques like a heuristic-based initialization, a path-relinking-based crossover operator, a referenced local search, and a procedure to control the diversity of the population, followed by calibration of the parameters of the proposed MA by means of a design of experiments approach. Finally, a comparative

evaluation is conducted with the contemporary best performing algorithms for the blocking flowshop with makespan criterion, which justifies the effectiveness of the proposed MA algorithms over the other contemporaries.

A Distributed assembly permutation flow-shop scheduling problem is discussed by Lin and Shuai [15] which widely exists in modern supply chains and manufacturing systems. An effective hybrid biogeography-based optimization algorithm is proposed by the authors in this paper that integrates several novel heuristics with the objective of minimizing the makespan. Further, a novel local search method is designed based on the problem characteristics and included in the proposed algorithm scheme to further improve the outputs on 900 small-sized instances and 810 large-sized instances and validated to demonstrate the effectiveness of the proposed algorithm.

Benkalai et. al. [16] addresses the problem of scheduling a set of independent jobs with set-up times on a set of machines in a permutation flow shop environment. A metaheuristic known as the Migrating Birds Optimization is used by the authors for the minimization of the makespan. The authors present two versions of the algorithm, out of which, the first is a basic Migrating Birds Optimization and the second introduces some additional features. An extensive computational study is carried out to validate the efficiency of the proposed methods with some benchmark of instances. The authors found that the second version performs better and may be considered for solving real-world scheduling problems.

Deb et. al. [17] illustrates, a novel metaheuristic search algorithm namely rhinoceros search algorithm (RSA), which is inspired by rhinoceros' natural behaviour. The authors also relate the present proposal with their earlier proposal of another algorithm called elephant search algorithm. The authors show that RSA simplifies certain habitual characteristics of rhinoceros and stream-lines the search operations, thereby reducing the number of operational parameters required to configure the model as well as, is able to outperform certain classical metaheuristic algorithms. The RSA is also implemented on permutation flow-shop scheduling problem as well. Finally the authors also compare other optimization technique sand find some improvement of RSA over some of the existing topologies.

4. Conclusion

In this paper, we focus on the heuristic based flowshop scheduling which is justified because the optimized solution to the scheduling problem is supposed to take exponential time as it is an NP Hard problem. The primary focus of the survey is on the permutation flowshop variant. We have discussed various algorithms and their performances. In addition to the permutation flowshop problem, we have also discussed in details about the other flowshop variants such as continuous

flowshop scheduling and block flowshop scheduling. Many researchers have had tried to develop algorithms to minimize the makespan, total flow time of the above stated variants of scheduling problems. Being NP Hard type problem, they need more and more effective and efficient solutions. The future researchers can try to use evolutionary algorithms, some nature inspired algorithms to solve this type of scheduling problem.

References:

1. A. Allahverdi and T. Aldowaisan, Int. J. Prod. Econ. **77** (2002) 71.
2. G.H. Campbell et al., Manage. Sci. **16** (1970) B-630.
3. M. Nawaz et al., Omega **11** (1983) 91.
4. C.J. Ho, Eur. J. Oper. Res. **81** (1995) 571.
5. C. Wang, C. Chengbin, and P. Jean-Marie, Eur. J. Oper. Res. **96** (1997) 636.
6. C. Rajendran and Z. Hans, Eur. J. Oper. Res. **103** (1997) 129.
7. H.S. Woo and Y. Dong-Soon, Comput. Oper. Res. **25** (1998) 175.
8. A. Fink and V. Stefan, Eur. J. Oper. Res. **151** (2003) 400.
9. J.M. Framinan and R. Leisten, Omega **31** (2003) 311.
10. E. Taillard, Eur. J. Oper. Res. **64** (1993) 278.
11. J. Liu, and C.R. Reeves, Eur. J. Oper. Res. **132** (2001) 439.
12. K. Chakravarthy and C. Rajendran, Prod. Plan. Cont. **10** (1999) 707.
13. D. Laha and A. Chakravorty, Int. J. Adv. Manuf. Tech. **53** (2011) 1189.
14. Q. Pan et al., IEEE Trans. Auto. Sci. Engg, **10** (2012) 741.
15. J. Lin, and Z. Shuai, Comput. Indus. Engg. **97** (2016) 128.
16. I. Benkalai et al., Int. J. Prod. Res. **55** (2017) 6145.
17. S. Deb et al., Soft Comput. **22** (2018) 6025

Scientific Voyage
Vol. 1, No. 1,
Page 45-59 (2020)

SCIENTIFIC VOYAGE
ISSN: 2395-5546

ISSN: 2395-5546

A Study onCustomerSentiment Analysis ofCommuter Airlines using Twitter Data Mining

Arkadip Ray[1] and Samik Datta[2]

[1]*Department of Information Technology,*
Government College of Engineering & Ceramic Technology, Kolkata - 700010, WB, India
Email: arka1dip2ray3@gmail.com
[2]*Department of Computer Science & Engineering,*
Techno Engineering College, Banipur, Habra - 743233, WB, India
Email: samikdatta123@gmail.com

Sentiment mining has mainly been correlated with analysis of text to establish whether an entity is of positive or, negative polarity. Recently, sentiment mining has been broadened to focus on objects such as distinguishing objective from subjective intentions, and determining the cradles and topics of different opinions expressed in textual formats such as tweets, web blogs, message board reviews, and news. Enterprises can leverage the opinion polarity and sentiment topic recognition to achieve a deeper perspective of the drivers and the overall scope of sentiments. These insights can improve customer service, establish better brand image, and enhance competitiveness. This paper solely examines the trend of analysing consumer feedbacks given in Twitter for various US based Airlines. Researchers are applying data mining and machine learning tools to accommodate different business centric evaluations such as Customer Feedback Assessment, Airline Quality Control, and Consumer Loyalty Prediction etc. Various knowledge building tools (lexicon creation, feature extraction, polarity formation) are emphasized in this study.These are applied to process the raw twitter data into characterized sentiment blocks which determine consumer intuition for choosing desired airlines. Also, external metrics such as weather condition, airline punctuality and service, staff oversight are taken into consideration that impact customer conclusions. This paper succinctly looks through sentiment recognition algorithms with their data processing paradigm and finally possible future directions for improvement are discussed.

*Keywords:*Netnography, Airline Quality Rating, Twitter Data, Machine Learning

1. Introduction

The rise of social media and innovative Web 2.0 technologies have marked the beginning decade of the twenty-first century, enabling faster and better online networking. Kaplan et al. [1] define social media as “a group of Internet-based applications that build on the ideological and technological foundations of Web 2.0, and that allow the creation and exchange of user-generated content”. Social media comprises online social communities (e.g. Facebook, LinkedIn etc.), blogs, content communities (e.g. YouTube), and wikis (e.g. Wikipedia), social bookmarking, and news sites (e.g. Reddit).

The principal distinction between the “old Web” and social media is accessibility of free and easy-to-use online tools for content editing, publishing, sharing, bookmarking and classification that enable interactive exchanges between individuals and groups. Originally

stemmed to facilitate connecting online and distribution of content across the Web, social media quickly became a favoured public platform for sharing experiences with products and services. Consumer commentaries in social media are sought after information on internet which are characterized by their originality and genuineness. Consumers' own reviews of products, services and brands are highly regarded among online audiences. Customers are also willing to voice their disappointment openly with products and services via social media.

Increasing number of blogs, tweets, online polls, and groups offering suggestion on products/services from the first-hand consumer perspective have transformed social media into an enormous depository of information with immeasurable potential for processing and chronicling customer data. Using social media as a source of customer feedback conform the fact that customer commentaries are posted on the internet by users for other enthusiasts, forming an ideal environment for modest and discreetresearch into customer.

This enables the research on customer experiences, and relieves an examiner from the cumbersome process of formal service quality studies. Over the past decade, numerousmethods have been proposed for analysing social media content, from netnography studies to opinion-mining and natural-language processing. In the following section we will focus our discussion on the opinion-mining, also known as sentiment analysis, for analysing consumer insights in social media and to unveil the experiencescustomers encounter when dealing with various types of services and service providers.

2. Sentiment Analysis on Customer Opinion

Sentiment analysis involvedsignificant interest in recent studies, ensuring to deliver effectiveness in analysing subjective and unstructured online content, especially in the social media setting (i.e. products/service blog reviews, video posts, tweet feeds, etc.). Sentiment analysis is an analytical procedure for classifying pieces of text into clusters containing views on specific topics (Jacobson et al. [2]). Every opinion is characterized by its holder, its target and its polarity. Using natural language processing tools, text mining and computational linguistics, sentiment analysis permits researchers to classify subjects of opinions, categorise them according to the standpoints and decide their emotional subtext, thus permitting researchers to associate customer experiences with particular responses.

According to Deshpande et al. [3], the objective of opinion mining is finally to enable decision-making in the view of quality control and performance evaluation. Also, by processing "raw" consumer data shared via social media, the acquired acumen can be used as a handle for further strategic acts. The matters that consumers share in social media is often filled with emotions of happiness, frustration, disappointment, delight and other feelings about experiences with services and service providers. What makes sentiment analysis uniquely fascinating is the ability to transform unstructured online content (i.e. tweets, blog commentaries, etc.) into structured data that can be processed to reveal information about sentiment patterns and trends that affects customer insights.

The analysis involves not only the recognition of themes in the online content (text), but also their emotional polarity, its intensity and degree of prejudice. This gives prospect for researchers to isolate customer opinions about services and also to develop new ideas on how to enrich service qualities and attributes. Sentiment analysis is considered as valuable

technique for "customer experience analysis".Advocates of opinion mining claim that automated text mining is more effectual substitute for opinion analysis than conventional customer surveys (which are often time consumingand costly).Although blogs, review sites and forums are some of the finest sources of subject matters about customer opinions, recent study efforts have indicated to the prospects that Twitter yields for opinion mining research.

3. Twitterand Sentiment Analysis

Micro-blogging site Twitter is among the world's top ten social media channels in terms of registered users and daily visits. In 2012, more than 100 million users posted 340 million tweets a day, and the service handled an average of 1.6 billion search queries per day. As of 2018, Twitter had more than 321 million monthly active users [4]. Twitter is one of the most popular social media platforms for sharing information and receiving real time updates. Despite its brief format which allows posting messages of only 280 characters at a time and a pretty simplistic goal (i.e. to answer the question "Where are you?"), Twitter sustained as one of the most preferred social mediaapparatus for information sharing. Its popularity attracted many companies to not only get in touch with consumers for sharing publicity information, but also to interact with them in real time and deal with issues arising before, during or, after services.

In sentiment analysis, a relatively new trend concentrates on analysing Twitter feeds to make future projections about customer behaviour, to dissect the effects of individual events and to supervise public attitudes on various topics. When a user reacts to an event by tweeting, he/sheexhibits "information behaviour", which basically includes some emotions, judgments or,intentions and consequently exposes intuitivesentiments on the tweeted topic.While the scope of Twitter data sentiment analysis is still reticent, there is growing interest in Twitter as a source of wide-ranging consumer information. Researchers are still assessing various techniques to inspect Twitter feeds and to extricate meaningful information from them. The following sectionintroduces the study on sentiment analysis of Twitter datato assess customer experiences in the airline industry.

4. Literature Review onSentiment Analysis

4.1 Marshall et al. [5] have devised a framework that conceptualises micro blogging service of Twitter which has allowed for customers to provide their positive, negative and/or noncommittal sentiment and opinion about air travel. It merges the twitter, natural disaster and aviation communities – briefly 4 U.S.-based severe weather events that included tornadoes, hurricane and massive snowstorm (called a nor'easter), 6 large and medium sized airlines and 3 weather stations. Through their evaluation, it is observed how a suite of keywords correlated to the weather event geographically and the timelines of the notification from the weather service affects airlines' services. In its proposed Flight Data Analyser framework, primacy of flight-related data on twitter in order to determine a commercial airline's quality of service to its customers in a significant weather event is optimized as main objective. The components are distributed in 4 modules –

- Designing a completely java-based modular framework for collecting, warehousing and processing flight-related data on twitter.
- Creating a semi-automated process to correlateeach weather event with an airline called the Fetcher Module. Twitter accounts of Airlines and weather services are sourced to identify relevant and accessible twitter data.
- Associating the weather conditions with the gathered tweeted content through Post-Filter and Analyser Modules.
- Testing the performance of Flight Data Analyser framework through the Performance Module, which provides basic statistics about tweets and run time of the Analyser Module.

Twitter Keywords	Targeted U.S. Airlines	Weather Events	Weather Services
airline, flight, delay, delivered, plane, airplane, weather, forecast, airport, schedule, cancelled, reschedule, postponed, postpone, take off, boarding, luggage, bag, bags, on time, October Snowstorm, Hurricane, Irene, disaster.	American, Delta, United, Southwest, JetBlue, Spirit	April 25-28, 2011 Tornado Outbreak, Joplin, Missouri Tornado (May 2011), Hurricane Irene (August 2011), Halloween Nor'easter (October 2011)	The Weather Channel, AccuWeather, National Oceanic and Atmospheric Administration (NOAA)

TABLE I – FLIGHT DATA ANALYSER FRAMEWORK DATASET

This system evaluates quality of service (QOS) measures by airlines through Performance Module.QOSinstruments took the form of number of retweets, relevancy of tweets, number of replies to customer tweets, and the Analyzer Module execution time. The retweet count signifies the efficacy of a particular tweet since the users would retweet only those that are suitable and pertinent. Tweet relevancy is the ratio of post-filtered tweets from the total tweets gathered with the pre-defined keywords. The number of replies to customer's tweets reveals airline customer service and how quickly they are posting replies to customer's concerns. From analysis of QOS, it is observed that American Airlines is very active on twitter in terms of replying to customer tweets but they lack in posting germanetweets in general. United Airlines delivers many useful tweets regarding flights, weather events etc., but performs poorly in terms of replying to tweets from customers. United Airlines is also observed to have a high ratio of relevant tweets. It is also the first airline under consideration to start web presence through twitter. Therefore, it is evident to infer that United Airlines has an edge over the other airlines in terms of twitter presence and customer service.

4.2 Misopoulos et al. [6] present a study that uses Twitter to identify critical elements of customer service in the airline industry. The goal of the study was to disclose customer opinions about services by supervising and analysing public Twitter commentaries; to identify components of customer service that deliver positive experiences to customers; to

pinpoint service processes and features that require further improvements.The authors employed the approach of sentiment analysis as part of the netnography study. The authors processed 67,953 publicly shared tweets to identify customer sentiments about services of four airline companies. Sentiment analysis was shepherded using the lexicon approach and vector-space model for assessing the polarity of Twitter posts.The sentiment analysis of the collected Twitter data began with the classification of tweets. Two approaches were used to categorise the tweets according to their content, in order to prepare them for further processing and assessment of sentiment polarity. All gathered tweets were grouped into three pools data, based on whether their subject matter included the keywords mentioned in Table II.

Sentiment categories	Representative words/symbols
Positive sentiment	"good," "awesome," "excellent," "best," "fine," "finest," "greatest," "ideal," "perfect," "top"
Negative sentiment	"fail," "bad," "weight," "delay," "failure," "lost," "sucks," "worst," "charge," "problem"
Neutral sentiment	"take," "fly," "airport, "find"

TABLE II – SENTIMENT MAPPED WITH KEYWORDS

Using the lexicon, the analysis is done by calculating the frequency of positive, negative, and neutral words/symbols in each tweet to define its polarity (i.e. positive, negative, or neutral). Vector Space Model (VSM) of information mining is implemented where each Tweet is represented as a vector and each dimension of the vector tallies with a separate term. The lexicon developed in this study consists of 20 terms (keywords), meaning that each tweet, represented as a vector, has 20 dimensions. In "document indexing," the first of the three stages of VSM, words without any relevant meaning to the content are discarded (i.e. the words "a" or "the"). In the second stage called "term weighting," the frequency of occurrence is calculated for each term (dimension). Using the lexicon, polarity scores are allocated to each word in the lexicon. In the third stage of VSM called "similarity coefficient," the query benchmarks are matched with the terms (keywords) within a tweet, thus indicating similarities.

By analysing Twitter posts for their sentiment polarity the authors are able to identify areas of customer service that caused customer satisfaction, dissatisfaction as well as delight. Positive sentiments are linked mostly to online and mobile check-in services, favourable prices, and flight experiences. Negative sentiments revealed problems with airlines' web sites, flight delays and lost luggage. Similarly, the approach revealed service features and practices that produced positive sentiments among customers (e.g. check-ins via mobile phone applications, good ticket prices, on-board entertainment, use of social media, etc.) and even testimonies of delightful service experiences (e.g. iPad access in lounges). Another interesting insight states that customers of airlines are eager to share both positive and negative aspects of their service experiences, and are often directly addressing companies with requests to address their problems. This proactive stance on customers' behalf to raise awareness about service problems obliges airlines for improved amenities.

4.3 Adeborna et al. [7] propose a sentiment mining approach which detects sentiment polarity and sentiment topic from text. The approach includes a Sentiment Topic Recognition (STR) method that is based on Correlated Topics Model (CTM) with Variational Expectation-Maximization (VEM) algorithm. The efficiency of this model is validated using airline data from Twitter. It also examines the reputation of three major airlines by computing their Airline Quality Rating (AQR) based on the output from the before mentioned approach.

The proposed methodology serves as an intelligent tool to answer questions regarding the drivers and overall scope of sentiments. The STR model is used to examine available data and to determine the reputation of airlines by computing their Airline Quality Rating (AQR). The AQR assessment is based on customer sentiments towards three major airlines (AirTran Airways, Frontier and SkyWest Airlines) accumulated from Twitter. An algorithm is developed to match opinionated tweets to a topic lexicon and an example of how the paradigm works is illustrated using a case study with real world tweets.

The case study includes classifying tweets for three airlines (AirTran, Frontier and SkyWest) as positive, neutral or negative. Then the proposed STR model is used to generate topics for each airline classified under four AQR categories (OT, DB, MB and CC). The tweets used in this experiment contain 452 tweets on AirTran, 499 on Frontier Airlines and 195 on SkyWest Airlines. Naïve Bayes Algorithm is employed which performed better on subjectivity dataset and provided a polarity classification accuracy of 86.4%. There are more positive tweets for AirTran than negative tweets, 57.5% and 27.6% respectively, the remaining being neutral. Frontier has 64.1% positive, 18.0% negative tweets and the rest are neutral. The overall sentiment score for SkyWest airline is highly positive with 82% tweets. SkyWest has approximately 19.4% negative tweets and remaining tweets are neutral (percentages are approximated).

STR model employs the CTM with VEM algorithm to generatelexicons from the airline tweets which are used in building each AQR category. In total, four lexicons are derived – on-time, denied boarding, mishandled baggage and customer complaint lexicons. This model yields better comparative performance to other STR models because the dependency and correlation between sentiment topics are taken into consideration. The STR model helps to rightly sort topic related terms under each AQR criteria for positive and negative polarity.

4.4 Duan et al. [8] built a model for six major U.S. airlines that executes sentiment analysis on customer reviews so that the airlines can have fast and concise feedback; make recommendations on the most important aspect of services they could improve given customers' complaints. The authors performed multi-class classification using Naive Bayes, SVM and Neural Network on US Airline Twitter data set collected from Kaggle.

The data set contains about 15,000 tweets collected in 2015 on various airline reviews. Every review is labelled as either positive, negative or neutral. The sentiment analysis labels are positive (20%), negative (60%), and neutral (20%). The negative reason labels are bad flight (7.45%), cancelled flight (9.62%), customer services issues (39.77%), damaged luggage (0.84%), flight attendant complaints (6.05%), flight booking problems

(6.19%), late Flights (1.99%), long lines (19.97%), and lost luggage (8.23%). In the data set, about 80% of the negative reviews has a negative reason label, yet the rest islabelled as "can't tell". By knowing every review's negative reason, specific suggestions can be given to different airline companies on how to improve their service.Sentiment Analysis and Negative Reason Prediction are the pillars of this model. For both tasks, Naive Bayes, SVM and Neural Network are used on the frequency matrix generated from the twitter dataset.

Naive Bayes with multinomial event model from 'sklearn' is used where input is the Laplace smoothed frequency vector. For Support vector machines, linear kernel and RBF kernel are used. SVM uses the same input and implementation package as Naive Bayes. Tensorflow is used in Neural Network implementation where input is the frequency vector that represents a review. The output is a vector with probabilities for different classes and the highest is selected as prediction. Furthermore Recurrent Neural Network which is a Bi-directional Gated Recurrent Unit Network (GRU) is used to capture the structure features of pre-trained word vectors that are trained on twitter data set. Also, it solves the vanishing gradient problem that many recurrent neural network models have.

In sentiment analysis, SVM with linear kernel achieves the best test accuracy. Therefore, SVM is recommended in this section. According to the result from linear SVM, Virgin American performs the best according to its lowest negative review composition in its total reviews. Given by the result of lowest test error, Naive Bayes is used for the prediction of unclassified data. From the results, it is clear that SVM and Naive Bayes perform better than deep learning methods. By associating major negative reasons for each airlines and airlines performance on service issues, negative reasons are classified as shown in the following table.

Airline	**1st Negative Reason**	**2nd negative Reason**
Virgin America	Customer Service Issue	Flight Booking Problems
United Airlines	Customer Service Issue	Late Flight
Southwest	Customer Service Issue	Late Flight
Delta	Late Flight	Customer Service Issue
US Airways	Customer Service Issue	Late Flight
American Airline	Customer Service Issue	Late Flight

TABLE III – AIRLINE WISE NEGATIVE SENTIMENT CLASSIFICATION

4.5 Hakh et al. [9] applied SMOTE method to analyse and solve the imbalanced challenge of the twitter datasets collected from US airline companies. In addition, the effect of feature selection and over-sampling techniques are tested on airline datasets. The "Twitter Airline Sentiment" dataset from Kaggle contains tweets covering six U.S. airline companies with 14,640 tweets, each of which is labelled according to sentiment polarity as: positive, negative, and neutral. In addition to the class label, all datasets share seven features namely Airline Sentiment, Airline Sentiment Confidence, Negative reason, Negative Reason Confidence, Airline, Retweet count, Text. Term frequency – Inverse Document Frequency (TF-IDF) is applied to measure weight of significant terms. Further, a tweet-term weight matrix is generated where the terms represent the features and weights are the TF-IDF scores calculated earlier.

In the first level of feature selection, genetic search is used as a filter to select the best subset of elements based on the correlation of features with the class label. In second level, a univariate feature selection process is applied which aimed at selecting the best subset of features based on statistical tests. The result portrays sentiment polarity of all the datasets, except for unevenly distributed data in Virgin America twitter handle. Unless solved, the training process of any classifier considering the imbalanced datasets will result in a bias due to the larger number of instances, sampled for training, and belonging to one class. Synthetic Minority Over-Sampling Technique (SMOTE) is added to increase the number of instances used for the training process from the minority class. Finally, on each of the partial datasets various classification techniques are applied (i.e. AdaBoost, Decision Tree, Linear SVM, Naïve Bayes, Random Forest, K-NN, and Kernel SVM) which aim at predicting the class of each tweet provided the subset of features are obtained after the two levels of feature selection and data balancing.

Classification settings per algorithm are set realistically after performing experiments with different settings. For example, number of trees in the random forest classifier is set to 4 as it showed the best results. On the other hand, the kernel chosen for the Kernel SVM is the Radial Basis Function (RBF). Additionally, for the K-NN classifier, the value of number of neighbours (k) are selected between 1, 3, and 5. Random Forest and Decision Tree have shown a high prediction level, and constancy when applied on all datasets. While K-NN and Linear SVM have shown an acceptable level of performance regarding all the evaluation metrics. On the other hand, Kernel SVM has shown poor results in comparison with other classifiers.

4.6 Joshi et al. [10] aims to provide a decision support for the customers for selecting the best fit US-based Airline, by presenting an Aspect level sentiment analysis on customer opinions available in micro blogging site Twitter and online review site Skytrax. This study supports a modified Knowledge discovery and data mining (KDD) methodology. Several machine learning algorithms (i.e. SVM, Decision tree, Random Forest, Bagging and Boosting, SLDA, Maximum Entropy) are applied in order to find out the best fit algorithm for the system.

The study follows a modified KDD methodology where a few stages are modified like implementation stage modified to Aspect and Sentiment Detection stage. The data for the research is taken from two sources, Twitter and online review site Skytrax. The assembled data was then interpreted as 1-gram, 2-gram and 3-gram manually by inspecting their frequency. Reviews are further categorized into five aspects (Food and Beverages services, Staff services, Luggage, Punctuality and Seat). A bag of words are added for each aspect after analysis of 1-gram and 2-gram. The polarity of each sentence isequated and a score isallocated for negative, neutral and positive as -1, 0 and 1 respectively.

Machine learning algorithms like support vector Machine (SVM), Glment, Maxent, SLDA, boosting, Random forest, neural networks and Decision Tree are applied and tested. The training and test dataset are separated in the ratio of 70:30. The final dataset consists attributes like cleaned sentence, polarity score, food and beverages aspect score, staff services score, luggage score, punctuality score and seat aspects score, airline names and airline code. This dataset is further treated for statistical operations to find out the correlations between the

different aspects and polarity score of the airlines. Also, linear regression is performed in order to find the connection between the attributes of the airlines.

The proposed algorithm is measured in terms of Precision, Recall, and F score. It is observed that Random Forest and Decision Tree performed well with the F-score of 0.60 resulting as the best fit algorithm.The first case study is an analysis of relation between three layers - Airlines, Aspects and Sentiments. United Airlines comes out to be 1st rank holder showing high positive response whereas Skywest Airline bags 10th rank with highest negative sentiments. The second case study is an analysis of aspects contribution towards the reviewer sentiments. From the unigram and word cloud implementation, "Seats", "Staff", "Punctuality", "Luggage" and "Food" are found to be the major areas of customer sentiments. The case study projects Seats Aspect as the most important aspect, whereas food is considered to be lowest contributor in the aspects towards customer's sentiments. Being one of the most popular airlines, United holds first rank in every aspect and there is a competitive edge between flights having mediocre ranking.

4.7 Ahuja et al. [11] focuses on identification of the diverse content typologies being used by Jet Airways on Twitter to implore Customer Engagement. This has been done, using a technique called Netnography. Subsequently, it proceeds to derive customer insights from the twitter page of Jet Airways, using wordclouds. The authors further attempt to generate aLexicon Based algorithm for Sentiment Analysis, using the tweets from the Jet Airways Twitter handle.

Netnography is a qualitative andexplanatoryresearch methodology that uses internet augmentedethnographic research techniques to study virtual networks and communities. Netnography is operatedon Twitter handle of Jet Airways and the analysis helps in distinguishingthe right type of content typology that will drawhigh levels of retweets and likes and successively more engagement from customers. A word cloud is a visual illustrationof text data, normallyused to portraykeyword metadata on websites. It represents the systemsupportedby a particular set of data (in this case twitter data) and is suggestiveof the ideaassociated with that set of textual information (tweets by customers of Jet Airways). The authors have generated word clouds to conduct a textual analysis using the Twitter handle of Jet Airways to extract social and customer insights from the content producedby the organisation and customers.Lexicon-based sentiment classification is possiblybe the most basic technique for computingthe sentimentpolarity of dataset (that is, a corpus). It needs a dictionary of words (a lexicon) which in this case is supplied from the Jet Airways Twitter handle and each word is then associated with Positive, Negative and Neutral polarity score.

Netnographic analysis of the Jet Airways Twitter page helps to extract the following Content Typologies - Organisational, Promotional and Relational Contents. The organisational content is not able to createadequate levels of customer retweets and likes (on an average). The promotional content increases customer interest in the brand. The relational content is able to generate a high level of retweets and likes. The word cloud, producedby at least 1500 tweets, depicts the service excellence that Jet Airways has attempted to achieve across the areas of punctuality, safety, seating comfort, large network, friendly and caring behaviour, professional and efficient staff, quality of food, cleanliness of the aircraft, quick baggage clearance, ease in booking tickets and easy check-ins.

4.8 Khaturia et al. [12] aim to provide a proper mechanism which helps the customers to opt for an airline in accordance to their comfortable experience. The process commenceswith collection of tweets on a large scale, analysing and classifying them as positive, negative and neutral – helps to delivera better rating and review which then assistthe customers to opt for achoiceas per their convenience.

The tweets generated from six major U.S. Airlines, namely Virgin, United, Delta, Southwest, American and US Airways are measuredas research data and the Sentiment Polarity Score for each airline is computedin order to rank them. Naïve Bayes Algorithm and Sentiment Analysis are applied on the classified tweets to create a comparative platform both statistically as well as graphically for the customer recommendation system.

After possessingtweets from Kaggle, they are categorized into three labels – positive, negative and neutral tweets. The subjects of negative tweets are mainly bad flights, cancelled flights, customer services issues, damaged or, lost luggage, flight attendant complaints, flight booking problems, late flights, long boarding lines etc. A feature matrix is then built to convert the textual information into numerical information. In the feature matrix, the number of rows indicates the number of samples, the number of columns indicates the length of the dictionary (i.e. collection of tweets), and each element indicates whether the specific word has appeared in the current review – "1" for existence and "0" for absence. Naïve Bayes classifiers are probabilistic units applied with Bayes' theorem for an applicableindependent assumption between its features (called naive). The classifiers are ascertainedfor every airline into positive, negative and neutral probabilities using the following formulas.

$$Score = \frac{positive + negative + neutral}{Total\,number\,of\,Tweets} \times 100$$

$$p(c \mid x) = \frac{p(x \mid c)p(c)}{p(x)}$$

Where p(c|x) is posterior probability, p(x) is predictor prior probability, p(c) is class Prior probability and p(x|c) is Likelihood.

Comparing the projectedscores of each airline, it is observed that Sentiment Analysis and Naïve Bayes Classification give contrasting results for Positive scores; for Neutral scores, both the algorithms provide similar result though the differences are quite high; the algorithms judge Negative scores with similar ratings. Evaluatingthe scores separately, one can predict the efficiency of the airlines based on which one can take the decision to choose an airline.

4.9 Ashi et al. [13] compared two word embedding models for aspect-based sentiment analysis (ABSA) of Arabic tweets. The ABSA instance isframedas a two-step process of aspect detection trailedby sentiment polarity classification of the detected aspects. The compared embedding models include fastText Arabic Wikipedia and AraVec-Web, both available as pre-trained models. Their corpus comprisedof 5K airline service related tweets in

Arabic, manually labelled for ABSA with imbalanced aspect categories. For classification, a support vector machine classifier is used for both aspect detection and sentiment polarity classification.The Arabic tweets dataset has the majority of tweets being in the Saudi dialect since the studied airline being the national carrier airline of Saudi Arabia.A distribution plot of the final dataset for the 13 specified aspects categories related to the airline service is performed manually by a group of native Arabic speakers.Also, for the study of sentiment polarity detection, the collected tweets are distributed regardingsentiment polarity. In this part of ABSA, the tweets are classified into projectedlabels either as positive (1410 tweets) or, as negative (3590 tweets), discarding the neutral tweets.

Aspect	Tweet Topics
Schedule	Flight schedule, rescheduling, timing, delays.
Destinations	Airline destination and routes.
Luggage and Cargo	Luggage, air cargo, luggage allowance, luggage delays.
Staff & Crew	All staff such as pilots and flight attendants.
Airplane	Airplane seating, cabin features, maintenance.
Lounges	First-class and frequent flyer service and airport lounges
Entertainment	In-flight entertainment, other media, and wi-fi.
Meals	In-flight meals and in-flight services.
Booking Services	Airline website, mobile app, and self-service machines.
Customer Service	Customer communications and complaint management
Refunds	Refund and compensations.
Pricing	Ticket pricing and seasonal airline offers.
Miscellaneous	It represents all tweets with gratitude and thanking or complaints about the airline in general.

TABLE IV – CATEGORY-WISE DISTRIBUTION OF OPINION ASPECTS

Employingthe two pre-trained word embedding models, simple vector-based features are used to classify the 5k collected airline-related tweets.By assessingthe semantic distance between Arabic words and phrases and byutilizing the Vector Space Mode, two defined sub-tasks are performed, namely Aspect Detection and Aspect-Based Sentiment detection. Two distinct word embedding models are utilized as the lexical resource for the two sub-tasks of Arabic aspect-based sentiment analysis. Such word embedding models utilisethe Vector Space Model (VSM) and cosine similarity between words.

Authors have trained a supervised SVM linear classifier using simple vector-based features on the labelled dataset to exploit it on unseen tweets to predict polarity – positive or, negative. For pre-training, two word embedding models are used, namely AraVec and fastText. Such vector-based features obtainboth semantic and sentiment information and these methods haveenhancedthe sentiment classification task.

This study also compares performance of two word embedding models using various evaluation metrics, namely, accuracy, precision, recall. The adopted pre-trained word embedding model used in both ABSA sub-tasks has performed comparably well in comparison to existing techniques. This vector space approach without any hand-crafted

features performs comparably well in comparison to techniques adopting manually engineered features.However, one limitation is thatthe dataset is imbalanced with a significant number of tweets between the 13 aspect classes as well as for the positive and negative polarity classes.

4.10 ---The research focus ofKhan et al. [14]is on analysis of tweets related to airlines based in four regions: Europe, India, Australia and America for consumer loyalty prediction. The tweets are used to calculate and graphically represent the positive, negative mean sentiment scores and a varying mean sentiment score over time for each airline. The terms for complaints and compliments are depicted using visualization methods. A novel method is proposed to measure and predict consumer loyalty using the data gathered from Twitter. Three classifiers are employed, namely, Random Forest, Decision Tree and Logistic Regression.They have collected tweets for 18 airlines based in four selected regions, which are America, India, Europe and Australia.Moreover, they have formed dataset for consumer loyalty analysis by collecting tweets using the search queries “loyal flyer”, “loyal to airline” as well as “left airline” totalling 10,000 tweets.

Airlines			
American	**European**	**Indian**	**Australian**
Delta, United, Spirit, Southwest, Jet Blue	Lufthansa, Air Berlin, Turkish Air, KLM, Easy Jet	Indigo, Air India, Jet Airways, Vistara, Spice Jet	Virgin, Qantas, Tiger Air, Jet Star, Sharp

TABLE V – AIRLINES TAKEN INTO CONSIDERATION

Sentiment Information Visualisation emphasises on user opinions posted on airline Twitter Help Desks or, on official Twitter handles of various airline companies.However, texts, images, links, emoticons and other forms of media that are present in a simple tweet create complications. Hence, the first step of the analysis is to clean the tweets and tokenize. Then sentiment analysis is operated on the tweets denotingmost positive, most negative and neutral. The mean scores of positive and negative sentiments are calculated for each airline. These scores areessentialfor an airline to realiseconsumer opinion about its services. An airline can make sure that its positive sentiment score is greater than negative sentiment score. Airlines may work to build their positive scores greater and negative scores lesser than their competitors. Brand sentiment score for a period of time is valuable for companies, since they indicate the positive attitude towards the brand or, the dissatisfaction with the same.

The positive terms are “awesome”, “excellent”, “delicious”, “perfect”, “superb” and “wonderful” with highest score of 1.0. The tweets with “worst” term expose the areas that need improvement and the positive tweets indicates to areas that are gaining appreciation and thus mandates an airline to keep up the good work.For Airline Passenger Loyalty, normalization is performed by dividing the difference between maximum and minimum loyalty score collected from the tweets using search queries such as “loyal flyer”, “loyal to airline” as well as “left airline”. The various values used to calculate the loyalty measurement are graphically represented in different combinations using the k-means clusters to illustrate the loyal and disloyal passengers.For consumer loyalty prediction, three prediction models

are used – Random Forest, Decision Trees and Logistic Regression. The model is fitted with positive and negative sentiment scores, mean of retweets, mean of likes and the number of followers. The models are tested on 10-fold cross validation and the maximum accuracy of 99.05% is observed for Random Forest.

Thus, identification ofcompliments and complaints, variations in sentiment over a period of time and mean sentiment score visualization provide passenger opinion on airline services. The consumer loyalty analysis assistsairlines to retain loyal flyers and bring in new customers.

4.11 Hong et al. [15] present a study that used text mining to develop a unified understanding of keywords in the aviation industry in a data-driven way. Based on the airline review data, it proposes a two-step process forobtainingkeywords using text mining and grouping them for cluster analysis.Particularly, it uses a combination of metrics and clustering algorithms to pre-process and analyse texts related to keyword extraction method, including text from the scientific literature and news articles. These keywords affect corporate marketing performance.

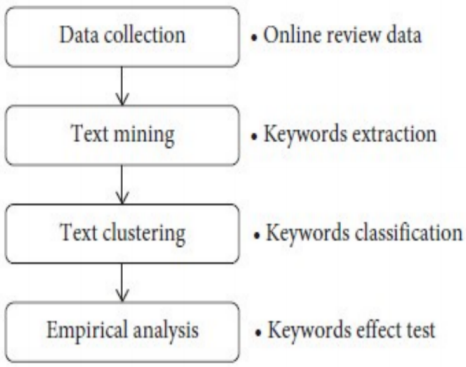

TABLE VI – FRAMEWORK OF DATA ANALYSIS

The authors have used the online review data from customers of two large air carriers in Korea and Japan, provided by global air service evaluation agency Skytrax in United Kingdom. One type of text data focuses on the customer experience with the airline services. The other type is the survey which include the evaluation of facilities, satisfaction, and recommendation after using the airline. Among the assembleddata, text data are used for core keyword extraction andquestionnaire data are used for practicalanalysis to verify the influence of core keywords. Text mining process is applied to extract words and text clustering process is utilised to analyse the collective sentiment of extracted words. Semantic analysis of the extracted 45 keywords is done where classification employed hierarchical clustering and the distance between the keywords are measured using the Euclidean method.

As a result of clustering analysis, 45 keywords aregroupedinto two clusters. Cluster 1 comprises of service content such as “seats”, “cabin”, “class”; “staff” who provides the service; service evaluation related keywords – “good”, “excellent”, “comfortable” etc. On the other hand, Cluster 2 contains more detailed service content such as “meal”, “movie”,

“drinks”, “check”, “served” etc. Also, it has service evaluation related keywords such as “great”, “nice”, “well”, “best”, “clean” etc.

Analysis shows“seats”, “staff” and “cabin”are positivelycorrelated withcustomer satisfaction and recommendation. It also shows that the airline customers talk frequently about “class” types (economy, business), but it does not influencethe customer satisfaction. This means that the airline should pay immediate attention to the seating arrangement in different classes along with continuing satisfactory performances in seat quality, staff attitude and cabinatmosphere.

5. Discussion on Recent Works

This study paper imparted an overview on the application of sentiment classification for better understanding of the airline commuter behaviour. The paper focuses on the different algorithms that have already been applied on the sentiment data for analysis. It also focuses on the proposed approach in depth, along with exploration of implementing tweet content in order to further improve the performance.

After going through the series of research work it is very clear that some supervised learning techniques produces good result. It is also seen that SVM or Naïve Bayes systems provide better result as compared to Neural Networks and Aspect-based decision support systems.Naïve Bayes and Support Vector Machines are the most frequently used machine learning algorithms for the purposes of sentiment classification. Many proposed algorithms are compared to these models as reference. But it is too early to judge that Neural Network will not produce better result.

Most of the research works emphasize either on attaining the sentiment polarity of customer experience or aim at deciding the rating or delay time of the airlines. Also, consuming Twitter feeds for three to four months is not sufficient in order to procure appropriate insights into customer behaviour towards airlines; so, there is a need for diversified data sets.

Transforming textual information into sentiment clusters provokes some genuine complications such as negative content processing, simplifying domains, language consideration and dealing with slangs or, profanity. Also, fake or spam reviews should be dealt with to eliminate ambiguity and opinionated results.

The articles presented in this survey mainly observes Twitter data generated in English language by customers of US based Airlines with few exceptions. To get a comprehensive understanding, all major spoken languages from Asian, European, Latin, Middle-East continents should be taken into consideration; the Natural Language Processing tools can be used to administer Sentiment Analysis.

6. Conclusion and Future Work

The objective of this paper is to review or, assemble the idea of sentiment analysis performed by different researcher in the domain of airline service using Twitter data. After analysing before mentioned articles, it is clear that the enhancement of current sentiment analysis algorithms is still a rewarding area of research.

Our future goal is to develop an ensemble of machine learning algorithms (supervised, unsupervised) and lexicon based approaches. By combining them with existing models, we are willing to identify areas of customer service that caused customer satisfaction, dissatisfaction as well as delight. This will be useful to rate major airlines by computing their Airline Service Quality (ASQ) and to build Airline Recommendation System based on customer feedbacks.Repository of data can be enriched by extending the data sources to social media (Facebook), online review sites (TripAdvisor, Skytrax, skyscanner, makemytrip) etc. The scope of customer sentiment modelling can be extended with advancement of data mining techniques into areas like automobile and railways.

REFERENCES

1. A. Kaplan and M. Haenlein, Business Horizons **53**, 59 (2010)
2. L. Jacobson, Public Relations Tactics **16**, 18 (2009)
3. M. Deshpande and A. Sarkar, Business Intelligence Journal **15**, 41 (2010)
4. www.wikipedia.com
5. B. Marshall et al., Journal of Emerging Trends in Computing and Information Sciences **3**, 8 (2012)
6. F. Misopoulos, M. Mitic, A. Kapoulas and C. Karapiperis, Management Decision **52**, 705 (2014)
7. E. Adeborna and K. Siau, Pacific Asia Conference on Information Systems (PACIS) Proceedings, Paper 363.
8. X.T. Duan, T. Ji and W. Qian, CS229, Stanford.edu (2016)
9. H. Hakh, I. Aljarah and B. Al-Shboul, Proceedings of the New Trends in Information Technology (NTIT-2017), The University of Jordan, Amman, Jordan
10. S. Joshi, "Aspect based sentiment analysis for United States of America Airlines", MSc Research Project – Data Analytics, School of Computing, National College of Ireland (2017)
11. V. Ahuja and M. Shakeel, Procedia Computer Science **122**, 17 (2017)
12. D. Khaturia et al., International Journal of Advanced Science and Technology **111**, 107 (2018)
13. M.M. Ashi, M.A. Siddiqui and F. Nadeem, Advances in Intelligent Systems and Computing **845** (2018)
14. R. Khan and S. Urolagin, International Journal of Advanced Computer Science and Applications **9**, 6 (2018)
15. J.-W. Hong and S.-B. Park, Hindawi Mobile Information Systems **8**, 1790429 (2019)